1

Polycyclic Aromatic Ketones – A Crystallographic and Theoretical Study of Acetyl Anthracenes

Sergey Pogodin, Shmuel Cohen, Tahani Mala'bi and Israel Agranat
Organic Chemistry, Institute of Chemistry, The Hebrew University of Jerusalem, Edmond J. Safra Campus, Jerusalem
Israel

1. Introduction

"Acylation differs from alkylation in being virtually irreversible" [Olah, 1973], free of rearrangements and isomerizations [Wang, 2009; Norman & Taylor, 1965]. This authoritative exposition of the state of the art of Friedel–Crafts chemistry in 1973 close to the centennial of the invention of the Friedel–Crafts reaction has been long recognized and not without reason. The difference in behavior between Friedel–Crafts acylation and Friedel–Crafts alkylation was attributed to the resonance stabilization existing between the acyl group and the aromatic nucleus [Buehler & Pearson, 1970], which may serve as a barrier against rearrangements and reversible processes. However, if the acyl group is tilted out of the plane of the aromatic nucleus, e.g., by bulky substituents, the resonance stabilization is reduced and the pattern of irreversibility of Friedel–Crafts acylation may be challenged [Buehler & Pearson, 1970; Pearson & Buehler, 1971; Gore, 1974]. Under these conditions deacylations and acyl rearrangements become feasible [Buehler & Pearson, 1970; Pearson & Buehler, 1971; Gore, 1974].

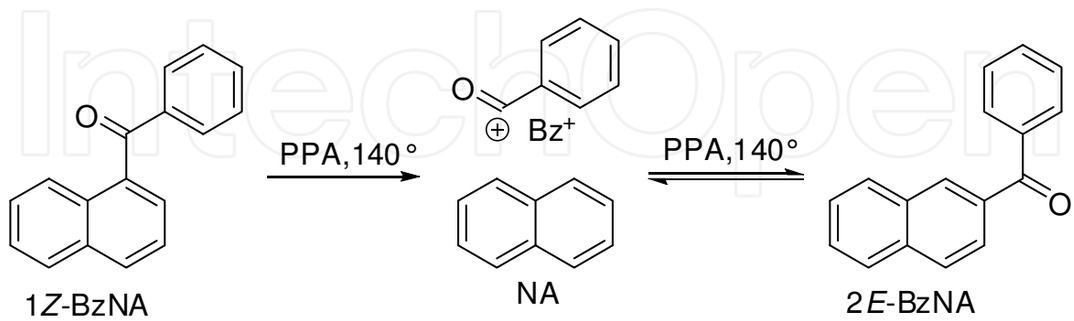

Fig. 1. The Friedel–Crafts acyl rearrangement of 1- and 2-benzoylnaphthalenes in PPA

The concept of reversibility in Friedel–Crafts acylations [Gore, 1955, 1964] was put forward in 1955 by Gore, who proposed that "the Friedel–Crafts acylation reaction of reactive hydrocarbons is a reversible process" [Gore, 1955]. Gore concluded that "Reversibility is an important factor in acylation reactions" [Gore, 1955]. The reversibility studies have been

focused mainly on unusual aspects of selectivity, including deacylations, one-way rearrangements and kinetic versus thermodynamic control [Gore, 1974]. Under classical Friedel–Crafts conditions (e. g., $AlCl_3$ and a trace of water), the pattern of irreversibility (e. g., in the naphthalene series) has been highlighted [Gore, 1964, 1974; Andreou et al., 1978; Dowdy et al., 1991].

The incursion of reversibility in Friedel–Crafts acylations was revealed by Agranat, et al. in the benzoylation of naphthalene in polyphosphoric acid (PPA) at elevated temperatures (Fig. 1) [Agranat et al., 1974]. The kinetically controlled 1-benzoylnaphthalene rearranged to the thermodynamically controlled 2-benzoylnaphthalene (PPA, 140 °C) (*vide infra*). The reversibility concept was then applied to the synthesis of linearly annelated polycyclic aromatic ketones by intramolecular Friedel–Crafts rearrangements of their angularly annelated constitutional isomers [Agranat & Shih, 1974a; Heaney, 1991]. The Haworth synthesis of PAHs, which previously had allowed access to angularly annelated PAHs could thus be applied to the synthesis of linearly annelated PAHs [Agranat & Shih, 1974b]. Further experimental evidence in support of true reversibility of Friedel–Crafts acylation is limited [Frangopol et al., 1964; Balaban, 1966; Nenitzescu & Balaban, 1964; Effenberger et al., 1973; Levy et al., 2007; Mala'bi et al,. 2009; Titinchi et al., 2008; Adams et al., 1998; Okamoto & Yonezawa, 2009]. Notable cases are the report by Balaban [Frangopol et al., 1964; Balaban, 1966; Nenitzescu & Balaban, 1964] on the reversibility of Friedel–Crafts acetylation of olefins to β-chloroketones, the report by Effenberger [Effenberger et al., 1973] of the retro-Fries rearrangement of phenyl benzoates (CF_3SO_3H, 170 °C) and the reversible ArS_E aroylation of naphthalene derivatives [Okamoto & Yonezawa, 2009]. Additional examples are the acyl rearrangements of acetylphenanthrenes [Levy et al., 2007] and acetylanthracenes [Mala'bi et al., 2009] in PPA, the acetylation of fluorene [Titinchi et al., 2008], the disproportionation of 9-acetylanthracene into 1,5- and 1,8-diacetylanthracenes in an ionic liquid systems [Adams et al., 1998]. Complete reversibility of Friedel–Crafts acylation was established in the intramolecular *para* $\rightleftharpoons$ *ortho* acyl rearrangements of fluorofluorenones in PPA (Fig. 2) [Agranat et al., 1977]. Friedel–Crafts acyl rearrangement of polycyclic aromatic ketones (PAKs) has been referred to as the Agranat–Gore rearrangement [Levy et al., 2007; Mala'bi et al., 2009]. The Friedel–Crafts acylation can be adjusted to give a kinetically controlled ketone or a thermodynamically controlled ketone [Buehler & Pearson, 1970]. Acyl rearrangements and reversibility in Friedel–Crafts acylations have been associated with thermodynamic control [Pearson & Buehler, 1971; Andreou et al., 1978; Agranat et al., 1977]. The contributions of kinetic control vs. thermodynamic control in Friedel–Crafts acyl rearrangements remain an open question, in spite of the rich chemistry of Friedel–Crafts acylations. We have recently shown that kinetic control wins out over thermodynamic control in the Friedel–Crafts acyl rearrangement of diacetylanthracenes in PPA [Mala'bi et al., 2011].

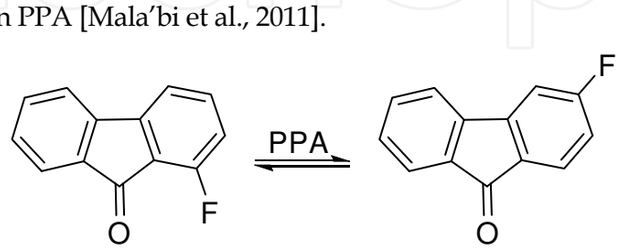

Fig. 2. The Friedel–Crafts intramolecular acyl rearrangements of fluorofluorenones in PPA

A plausible mechanism of the Friedel–Crafts acyl rearrangement of 1-benzoylnaphthalene (1-BzNA) into 2-benzoylnaphthalene (2-BzNA) in PPA, is presented in Fig. 3. The

mechanism involves the two dibenzoylnaphthalenes, their *O*-protonates and their σ-complexes. In the kinetically controlled pathway 1σ-BzNAH$^+$ is more stable than 2σ-BzNAH$^+$ and by virtue of the Hammond–Leffler postulate [Muller, 1994] the transition state leading to 1σ-BzNAH$^+$ is lower in energy than the transition state leading to 2σ-BzNAH$^+$. Thus, 1-BzNA is the kinetically controlled product. By contrast, in the thermodynamically controlled pathway, 1-BzNAH$^+$ and 1-BzNA are less stable than 2-BzNAH$^+$ and 2-BzNA, respectively. Therefore, 2-BzNA is the thermodynamically controlled product. Under conditions of thermodynamic control, the relative stabilities of the constitutional isomers of a given PAK are detrimental to the products of the Friedel–Crafts acyl rearrangement of the PAK and of the Friedel–Crafts acylation of the corresponding PAH.

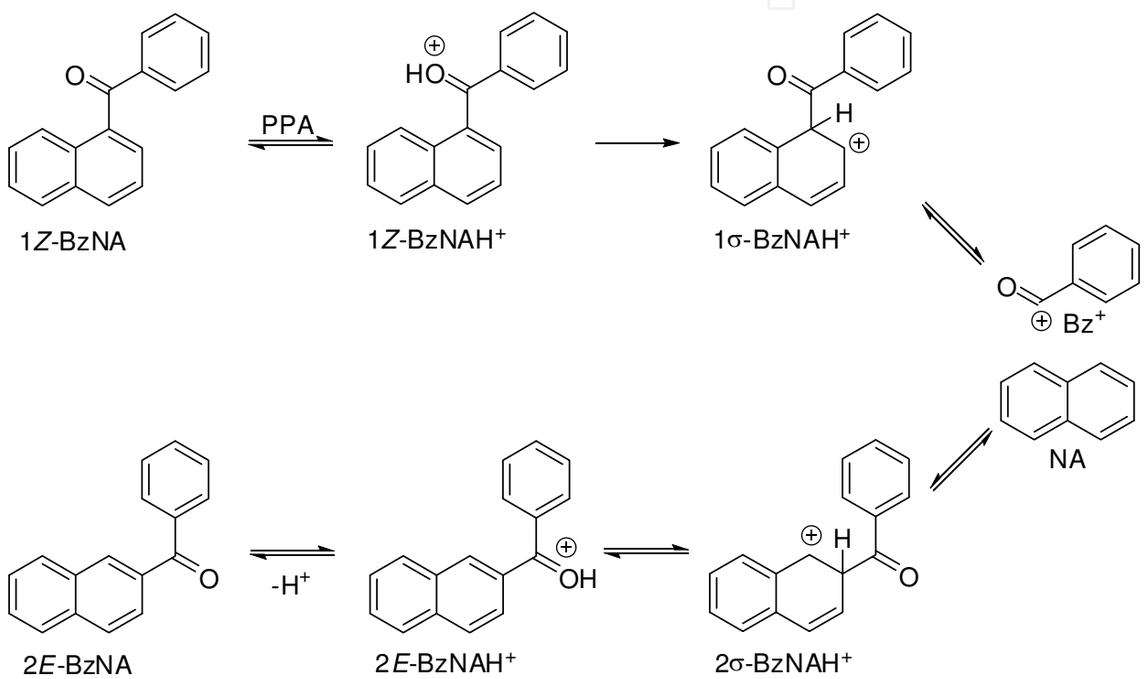

Fig. 3. The mechanism of the Friedel–Crafts acyl rearrangement of representative PAKs 1- and 2-benzoylnaphthalenes.

2. Structures of monoacetylanthracenes and diacetylanthracenes

Anthracene (AN) is essentially a planar PAH. Due to its D_{2h} symmetry, three constitutional isomers of acetylanthracenes (AcAN) are possible: 1-acetylanthracene (1-AcAN), 2-acetylanthracene (2-AcAN), and 9-acetylanthracene (9-AcAN) (see Fig. 4). These isomers differ in the position of the acetyl substituent at the anthracene ring system. The three constitutional isomers of AcAN can be categorized, depending on the degree of their overcrowding: (i) the non-overcrowded isomer 2-AcAN, in which the acetyl group is flanked by two *ortho*-hydrogens (H^1, H^3); (ii) the overcrowded isomer 1-AcAN, in which the overcrowding is due to the presence of one hydrogen atom (H^9) *peri* to the acetyl group; (iii) the severely overcrowded isomer 9-AcAN (assuming the planar conformation), in which the overcrowding is due to the presence of two *peri*-hydrogens (H^1, H^8) to the acetyl group. The

overcrowding in 1-AcAN and 9-AcAN should result in significant deviations of the acetyl groups from the plane of the anthracene nucleus, which is expected to encourage reversibility and rearrangements.

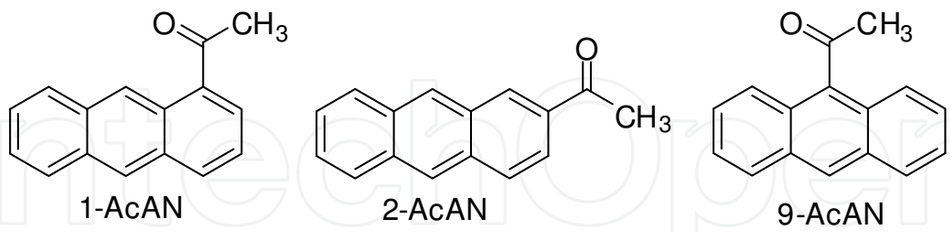

Fig. 4. Constitutional isomers of monoacetylanthracenes (*E* and *Z* stereodescriptors are omitted)

There are 15 constitutional isomers of diacetylanthracenes (Ac_2AN), shown in Fig. 5. These isomers differ in the position of the acetyl substituents at the anthracene ring system. The present study encompasses the three monoacetylanthracenes 1-AcAN, 2-AcAN, 9-AcAN and the following eleven diacetylanthracenes: 1,5-Ac_2AN, 1,6-Ac_2AN, 1,7-Ac_2AN, 1,8-Ac_2AN, 1,9-Ac_2AN, 1,10-Ac_2AN, 2,6-Ac_2AN, 2,7-Ac_2AN, 2,9-Ac_2AN, 2,10-Ac_2AN and 9,10-Ac_2AN. The remaining diacetylanthracenes, 1,2-Ac_2AN, 1,3-Ac_2AN, 1,4-Ac_2AN and 2,3-Ac_2AN were not included in the present study. These constitutional isomers are not expected to be formed in the Friedel–Crafts acylations of 1-AcAN and 2-AcAN, due to the deactivation effect of the electron-withdrawing acetyl group towards further acetylation. This effect is not necessarily operating with respect to the "remote" unsubstituted benzene ring.

In 1-AcAN and 2-AcAN, the *E*- and *Z*-diastereomers should be considered. *E* and *Z* are the stereodescriptors applied to monoacetylanthracenes and diacetylanthracenes with a fractional bond order of the bond between the carbonyl carbon and the corresponding aromatic carbon [Moss, 1996]. In diacetylanthracenes, four diastereomers should be considered: *ZZ*, *ZE*, *EZ* and *EE*. Depending on the symmetry of a given diacetylanthracene, *ZE* and *EZ* diastereomers could be equivalent. 9,10-AcAN is a special case: only one stereodescriptor, *Z* or *E*, is required. In this case, *Z* or *E* refers to whether the carbonyl bonds lie on the same or on the opposite sides of the plane containing the C^9–C^{11} and C^{10}–C^{12} bonds and perpendicular to the aromatic plane.

Acetylanthracene 2-AcAN and diacetylanthracenes 1,5-Ac_2AN, 1,6-Ac_2AN, 1,7-Ac_2AN, 1,8-Ac_2AN, 2,7-Ac_2AN and 9,10-Ac_2AN have been synthesized in the present study and their crystal structures have been determined. Ketones 2-AcAN, 1,5-Ac_2AN and 1,8-Ac_2AN have been prepared by the Friedel–Crafts acetylation of anthracene. Ketones 1,6-Ac_2AN, 1,7-Ac_2AN and 2,7-Ac_2AN have been prepared by the Friedel–Crafts acetylation of 2-AcAN. Ketone 9,10-Ac_2AN has been synthesized by methylation (MeLi) of 9,10-dicarbomethoxyanthracene (prepared from 9,10-dibromoanthracene via 9,10-anthracenedicarboxylic acid). Ketones 1,7-Ac_2AN and 2,7-Ac_2AN are reported here for the first time.

The present study encompasses the crystal and molecular structures of monoacetylanthracenes (AcANs) and diacetylanthracenes (Ac_2ANs), the results of a systematic DFT study of the structures and the conformational spaces of AcANs and Ac_2ANs, as well as the comparison between the calculated and the experimental structures of these PAKs.

2.1 Molecular and crystal structure of monoacetylanthracenes and diacetylanthracenes

Of the three monoacetylanthracenes and eleven diacetylanthracenes included in the present study, only the crystal structures of 1-AcAN [Langer & Becker, 1993], 9-AcAN [Anderson et al., 1984; Zouev et al., 2011] and 1,5-AcAN [Li & Jing, 2006] have previously been described. The molecular and crystal structures of 2-AcAN, 1,6-Ac_2AN, 1,7-Ac_2AN, 1,8-Ac_2AN, 2,7-Ac_2AN and 9,10-Ac_2AN are reported here for the first time, along with the previously reported structures.

2.1.1 Geometries of monoacetylanthracenes and diacetylanthracenes

Table 1 shows the crystallographic data for 2-AcAN, 1,5-Ac_2AN, 1,6-Ac_2AN, 1,7-Ac_2AN, 1,8-Ac_2AN, 2,7-Ac_2AN and 9,10-Ac_2AN.[1] The ORTEP diagrams of 2-AcAN and of the six diacetylanthracenes as determined by X-ray crystallography are presented in Fig. 6–10. Ketones 2-AcAN, 1,5-Ac_2AN, 1,8-Ac_2AN and 2,7-Ac_2AN crystallize in the monoclinic space groups $P2_1/n$, $P2_1/c$, $P2/n$ and $I2/a$, respectively. The unit cell dimensions of the crystal structure of 1,5-Ac_2AN are essentially identical to those reported in the literature [Li & Jing, 2006]. Ketones 1,6-Ac_2AN and 1,7-Ac_2AN crystallize in the triclinic space group P-1. Ketone 9,10-Ac_2AN crystallizes in the orthorhombic space group $Pna2_1$. Table 2 gives selected geometrical parameters derived from the X-ray crystal structures of the mono- and diacetylanthracenes under study. The following geometrical parameters were considered: the twist angles $\tau(C_{arom}–C_{arom}–C_{carb}–O)$ (divided into τ_1, τ_2 and τ_9 depending on the position of the acetyl group) and $\upsilon(C_{arom}–C_{arom}–C_{carb}–O)$ around the anthracenyl-carbonyl bond; the dihedral angle θ between the least-square planes of the carbonyl group and the anthracene system; the dihedral angle φ between the least-square planes of two side rings of the anthracene system; the pyramidalization angles χ at C_{arom} and C_{carb}. Table 3 gives the bond lengths in the mono- and diacetylanthracenes under study, as compared with the parent anthracene.

The data presented in Table 3 indicate the considerable variation in bond lengths in mono- and diacetylanthracenes. The bond lengths may be classified into several types: four $C^1–C^2$, or α-β, bonds (134.2–137.7 pm), two $C^2–C^3$, or β-β, bonds (138.7–144.4 pm), four $C^1–C^{9a}$ bonds (141.8–145.5 pm), four $C^{9a}–C^9$ bonds (138.3–140.9 pm), and two $C^{4a}–C^{9a}$ bonds (142.8–145.3 pm). These values are in the same range as the respective bond lengths in the X-ray crystal structure of anthracene, which are 136.1, 142.8, 143.4, 140.1 and 143.6 pm [Brock & Dunitz, 1990]. It has previously been shown that the bond lengths in anthracene are in agreement with the superposition of its four Kekulé structures and with the free valence numbers [Sinclair et al., 1950]. Table 3 also shows that the bonds adjacent to the acetyl group are elongated as compared to the respective bonds in anthracene, e.g. the $C^2–C^3$ bond in 2-AcAN (143.2 pm vs. 142.8 pm), the $C^1–C^2$ bonds in 1,5-Ac_2AN and 1,8-Ac_2AN (137.5 pm vs. 136.1 pm), the $C^5–C^6$ bonds in 1,6-Ac_2AN (137.0 pm vs. 136.1 pm), the $C^7–C^8$ bond in 1,7-Ac_2AN (137.4 pm vs. 136.1 pm) and the $C^2–C^3$ bond in 2,7-Ac_2AN (144.4 pm vs. 142.8 pm). This elongation effect stems from the contributions of dipolar Kekulé structures, in which the anthracene bonds adjacent to the acetyl group are necessarily single. This effect, however, is not noticeable in 9,10-Ac_2AN, because the carbonyl groups are almost perpendicular to the aromatic plane and are hardly conjugated with the anthracene system.

[1] CCDC 839159 – 839165 contains the supplementary crystallographic data for this paper. These data can be obtained free of charge from The Cambridge Crystallographic Data Centre via www.ccdc.cam.ac.uk/data_request/cif.

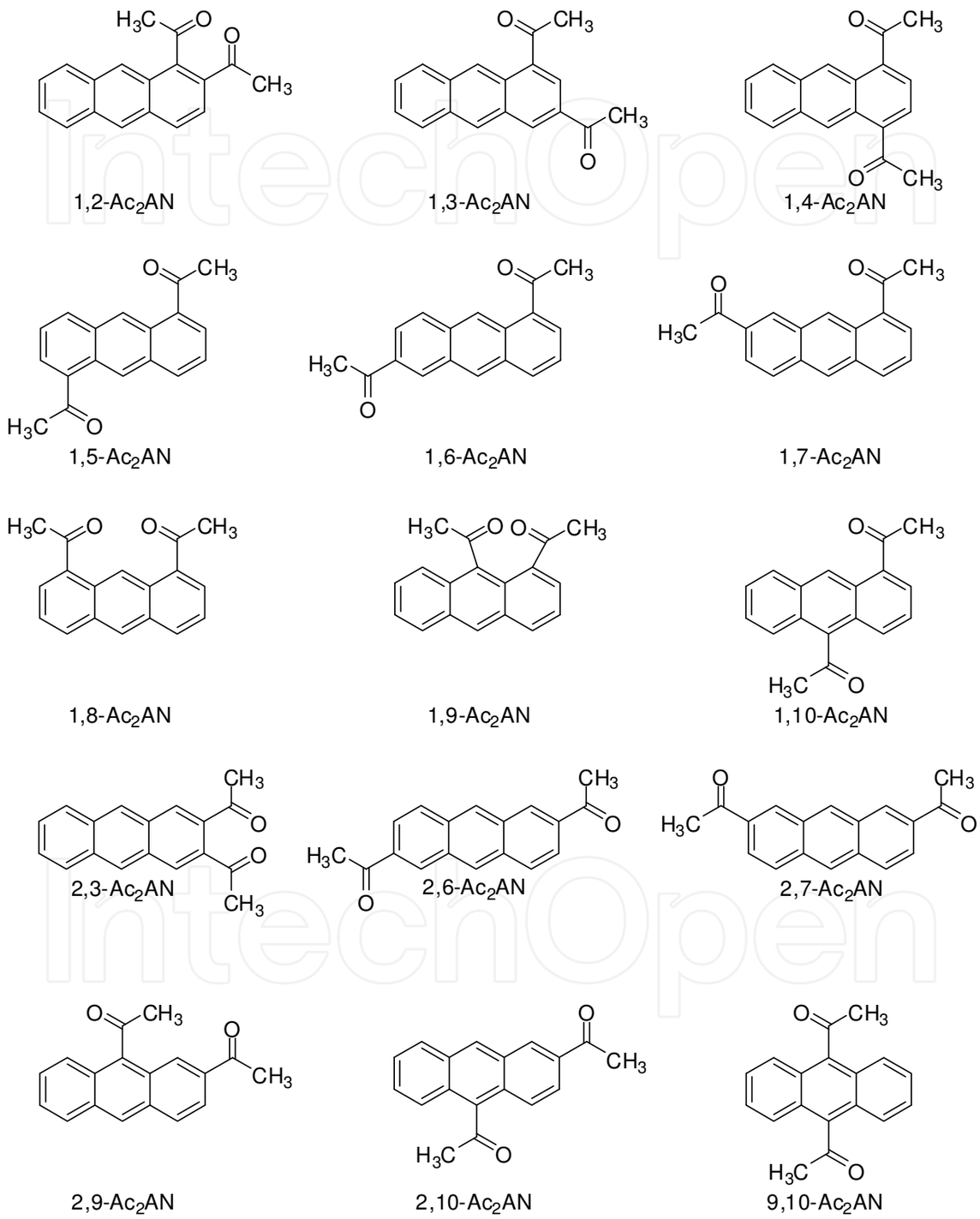

Fig. 5. Constitutional isomers of diacetylanthracenes (*E* and *Z* stereodescriptors are omitted)

	2-AcAN	1,5-Ac_2AN	1,6-Ac_2AN	1,7-Ac_2AN	1,8-Ac_2AN	2,7-Ac_2AN	9,10-Ac_2AN
Formula	$C_{16}H_{12}O$	$C_{18}H_{14}O_2$	$C_{18}H_{14}O_2$	$C_{18}H_{14}O_2$	$C_{18}H_{14}O_2$	$C_{18}H_{14}O_2$	$C_{18}H_{14}O_2$
Temp, K	173(1)	173(1)	173(1)	123(2)	173(1)	173(1)	173(1)
Crystal system	Monoclinic	Monoclinic	Triclinic	Triclinic	Monoclinic	Monoclinic	Orthorhombic
Space group	$P2_1/n$	$P2_1/c$	P-1	P-1	$P2/n$	$I2/a$	$Pna2_1$
a, Å	6.031(2)	9.8394(9)	7.5776(12)	7.9765(6)	12.6504(9)	17.003(4)	10.4235(14)
b, Å	7.394(3)	6.2073(6)	8.8581(14)	8.2802(6)	8.5008(6)	5.8390(13)	7.9835(10)
c, Å	24.847(9)	10.8876(10)	10.1653(16)	11.2321(8)	12.6756(9)	26.395(6)	16.164(2)
α, deg	90.0	90.0	92.062(3)	96.661(1)	90.0	90.0	90.0
β, deg	90.051	107.630(1)	94.348(3)	96.863(1)	108.605(1)	94.592(4)	90.0
γ, deg	90.0	90.0	110.604(3)	115.295(1)	90.0	90.0	90.0
Volume, $Å^3$	1108.07(7)	633.7(1)	637.9(2)	654.28(8)	1291.9(2)	2612.1(10)	1345.1(3)
Z	4	2	2	2	4	8	4
Calc density Mg/m^3	1.320	1.375	1.365	1.331	1.349	1.334	1.295
Crystal size							
max, mm	0.16	0.27	0.40	0.25	0.42	0.37	0.27
mid, mm	0.14	0.26	0.20	0.22	0.40	0.18	0.24
min, mm	0.06	0.23	0.15	0.13	0.28	0.09	0.17
Reflections collected	6443	6860	5077	7510	14485	14453	13845
Independent reflections	2581 R_{int}=0.0676	1494 R_{int}=0.0231	2875 R_{int}=0.0181	3033 R_{int}=0.0181	3089 R_{int}=0.0257	3124 R_{int}=0.0390	2936 R_{int}=0.0263
Reflections with I>2σ(I)	1307	1429	2336	2689	2841	2275	2865
Final R indices [I>2σI]	R_1=0.0880 wR_2=0.1803	R_1=0.0496 wR_2=0.1253	R_1=0.0583 wR_2=0.1498	R_1=0.0470 wR_2=0.1312	R_1=0.0705 wR_2=0.1847	R_1=0.0771 wR_2=0.1747	R_1=0.0510 wR_2=0.1242
R indices (all data)	R_1=0.1691 wR_2=0.2185	R_1=0.0518 wR_2=0.1271	R_1=0.0710 wR_2=0.1588	R_1=0.0523 wR_2=0.1362	R_1=0.0748 wR_2=0.1900	R_1=0.1051 wR_2=0.1896	R_1=0.0520 wR_2=0.1248

Table 1. Crystallographic data for acetylanthracenes 2-AcAN, 1,5-Ac_2AN, 1,6-Ac_2AN, 1,7-Ac_2AN, 1,8-Ac_2AN, 2,7-Ac_2AN and 9,10-Ac_2AN.

Compound			τ^a deg	υ^b deg	θ deg	φ deg	C_{carb}–$C_{an}{}^c$ pm	$\chi(C_{arom})$ deg	$\chi(C_{carb})$ deg	O···H pm		CH_3···H pm	
1-AcAN	*Z*	C_i	27.1	-152.7	28.6	3.2	149.3	-0.1	-0.2	223.4	H^9	223.4	H^2
2-AcAN	*E*	C_1	173.1	-5.3	5.9	0.4	148.6	-1.6	0.4	249.2	H^3	244.3	H^1
9-AcAN	--	C_1	87.9	-91.8	89.2	5.8	150.4	0.3	-0.8	294.0	H^1	263.1	H^8
1,5-Ac_2AN	*ZZ*	C_i	20.0	-156.8	22.7	0.0	149.4	-3.2	3.4	226.9	H^9	243.7	H^2
1,6-Ac_2AN	*ZE*	C_1	30.0	-147.1	32.2	1.3	150.1	-2.9	3.0	228.8	H^9	230.0	H^2
			178.6	-0.7	1.9		149.3	-0.7	-0.3	249.9	H^7	230.1	H^5
1,7-Ac_2AN	*ZE*	C_1	-15.2	162.9	16.0	2.3	149.8	1.9	-1.9	221.3	H^9	229.2	H^2
			-176.6	3.7	4.5		149.0	0.3	-0.6	247.9	H^6	229.5	H^8
1,8-Ac_2AN	*ZZ*	C_2	-34.0	145.4	36.0	0.3	149.3	0.6	0.3	228.2	H^9	231.1	H^2
			-32.4	144.9	35.4	3.4	148.9	2.7	0.2	225.9	H^9	226.7	H^2
2,7-Ac_2AN	*EZ*	C_1	171.9	-3.4	9.9	2.9	149.0	-4.7	3.0	253.9	H^3	239.0	H^1
			0.9	-178.5	2.0		148.9	0.7	-1.3	246.0	H^8	226.4	H^3
9,10-Ac_2AN	*E*	C_1	-85.0	94.0	86.7	1.6	151.3	-1.0	-1.2	288.2	H^8	257.4	H^1
			87.0	-93.7	86.5		151.5	-0.6	0.1	290.5	H^4	264.4	H^5

[a] $\tau_1(C^{9a}–C^1–C^{11}–O^{15})$ for 1-AcAN, 1,5-Ac_2AN, 1,6-Ac_2AN, 1,7-Ac_2AN and 1,8-Ac_2AN, $\tau_2(C^1–C^2–C^{11}–O^{15})$ for 2-AcAN and 2,7-Ac_2AN, $\tau_2(C^5–C^6–C^{13}–O^{16})$ for 1,6-Ac_2AN, $\tau_2(C^8–C^7–C^{13}–O^{16})$ for 1,7-Ac_2AN, $\tau_9(C^{9a}–C^9–C^{11}–O^{15})$ for 9-AcAN and 9,10-Ac_2AN.
[b] $\upsilon_1(C^2–C^1–C^{11}–O^{15})$ for 1-AcAN, 1,5-Ac_2AN, 1,6-Ac_2AN, 1,7-Ac_2AN and 1,8-Ac_2AN, $\upsilon_2(C^3–C^2–C^{11}–O^{15})$ for 2-AcAN and 2,7-Ac_2AN, $\upsilon_2(C^7–C^6–C^{13}–O^{16})$ for 1,6-Ac_2AN, $\upsilon_2(C^6–C^7–C^{13}–O^{16})$ for 1,7-Ac_2AN, $\upsilon_9(C^{8a}–C^9–C^{11}–O^{15})$ for 9-AcAN and 9,10-Ac_2AN.
[c] $C^1–C^{11}$ for 1-AcAN, 1,5-Ac_2AN, 1,6-Ac_2AN, 1,7-Ac_2AN and 1,8-Ac_2AN, $C^2–C^{11}$ for 2-AcAN and 2,7-Ac_2AN, $C^6–C^{13}$ for 1,6-Ac_2AN, $C^7–C^{13}$ for 1,7-Ac_2AN, $C^9–C^{11}$ for 9-AcAN and 9,10-Ac_2AN.

Table 2. Selected geometrical parameters of the X-ray molecular structures of acetylanthracenes 2-AcAN, 1,5-Ac_2AN, 1,6-Ac_2AN, 1,7-Ac_2AN, 1,8-Ac_2AN, 2,7-Ac_2AN and 9,10-Ac_2AN.

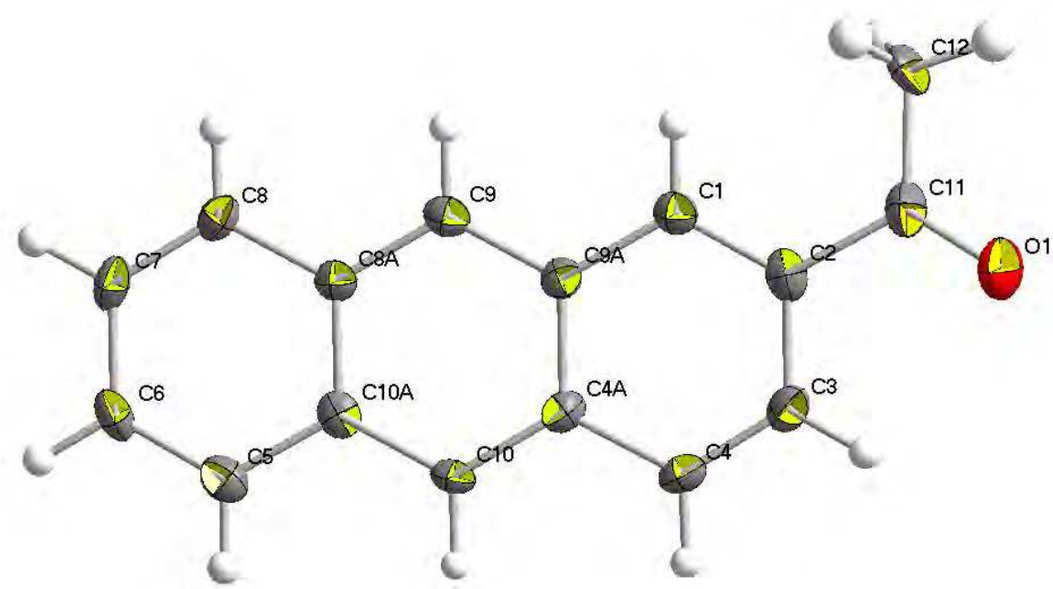

Fig. 6. ORTEP drawing of the crystal structure of 2-AcAN, scaled to enclose 50% probability

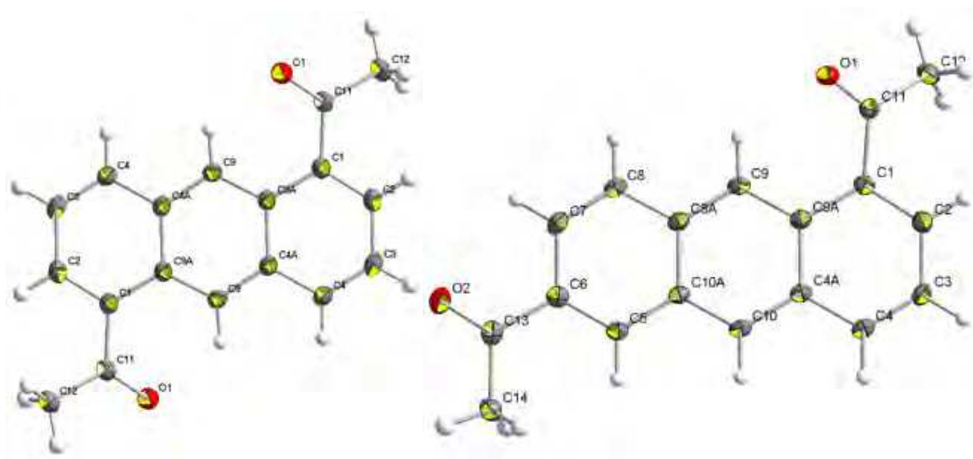

Fig. 7. ORTEP drawings of the crystal structures of 1,5-Ac_2AN (left) and 1,6-Ac_2AN (right), scaled to enclose 50% probability

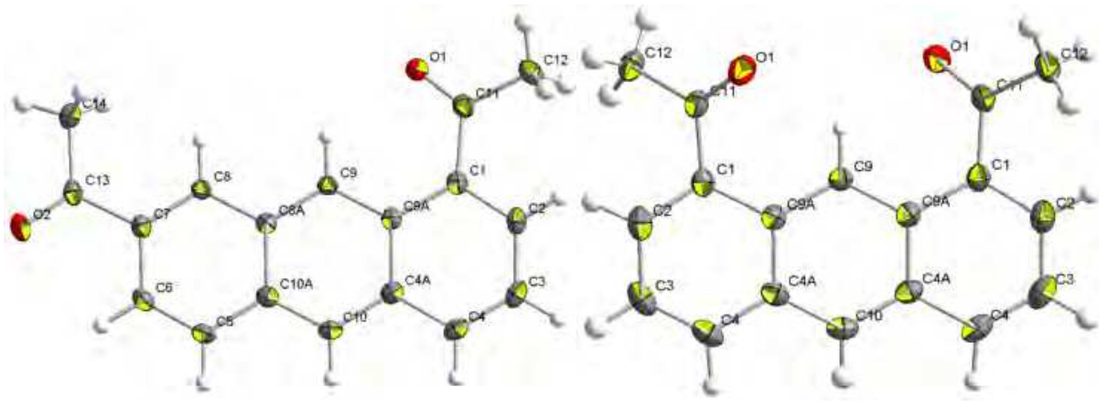

Fig. 8. ORTEP drawings of the crystal structures of 1,7-Ac_2AN (left) and 1,8-Ac_2AN (right), scaled to enclose 50% probability

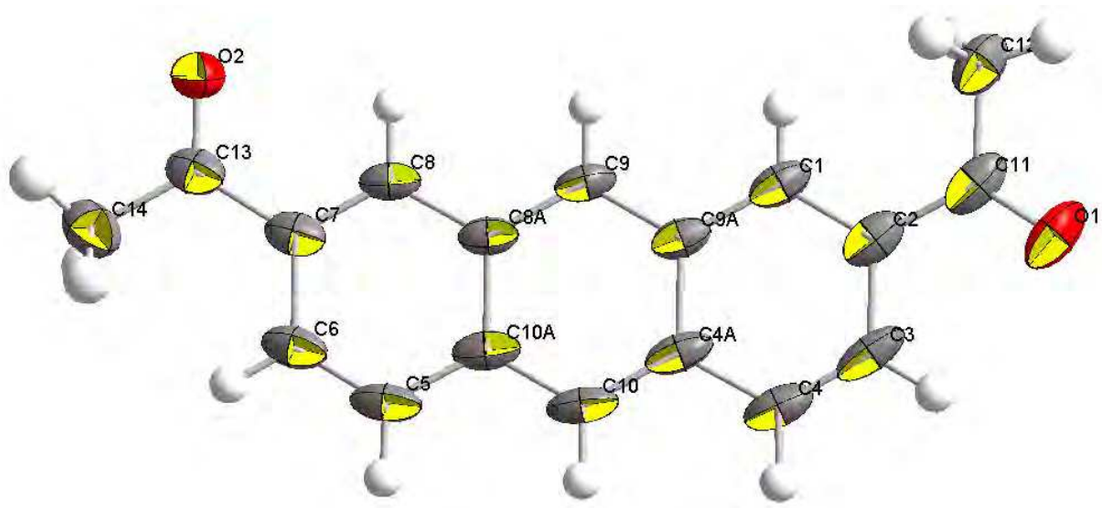

Fig. 9. ORTEP drawings of the crystal structure of 2,7-Ac_2AN, scaled to enclose 50% probability

	C^1–C^2	C^2–C^3	C^3–C^4	C^4–C^{4a}	C^{4a}–C^{9a}	C^{4a}–C^{10}	
AN[a]	136.1	142.8	136.1	143.4	143.6	140.1	
1-AcAN[b]	137.6(3)	138.7(3)	134.6(3)	143.1(3)	143.1(3)	139.2(3)	
2-AcAN	136.4(4)	143.2(4)	134.6(4)	144.10(4)	143.0(4)	138.7(4)	
9-AcAN[c]	134.9(3)	141.2(3)	135.0(3)	142.9(3)	143.2(3)	138.8(3)	
1,5-Ac_2AN	137.5(2)	141.4(2)	135.6(2)	142.9(2)	143.8(2)	139.9(2)	
1,6-Ac_2AN	136.9(2)	142.0(2)	135.5(2)	142.7(2)	144.1(2)	140.0(2)	
1,7-Ac_2AN	137.7(2)	141.5(2)	135.6(2)	143.0(2)	144.0(2)	140.0(2)	
1,8-Ac_2AN	137.3(2)	141.4(3)	135.5(2)	142.8(2)	143.7(2)	139.2(2)	
1,8-Ac_2AN	137.5(2)	141.2(3)	135.2(3)	142.9(2)	143.7(2)	139.2(2)	
2,7-Ac_2AN	137.1(3)	144.4(3)	134.2(4)	142.5(3)	144.6(3)	138.3(3)	
9,10-Ac_2AN	136.3(3)	141.8(4)	134.6(4)	142.7(3)	143.8(3)	140.9(3)	
	C^{10}–C^{10a}	C^{10a}–C^{8a}	C^{10a}–C^5	C^5–C^6	C^6–C^7	C^7–C^8	C^8–C^{8a}
AN[a]	140.1	143.6	143.4	136.1	142.8	136.1	143.4
1-AcAN[b]	139.5(3)	142.8(3)	143.0(3)	134.6(3)	140.8(3)	135.1(3)	142.2(3)
2-AcAN	139.3(4)	143.6(4)	142.4(4)	136.1(4)	141.3(4)	135.0(4)	143.0(4)
9-AcAN[c]	139.1(3)	142.9(3)	142.4(3)	134.5(3)	140.4(3)	135.6(3)	142.7(3)
1,5-Ac_2AN	139.7(2)	143.8(2)	145.0(2)	137.5(2)	141.4(2)	135.6(2)	142.9(2)
1,6-Ac_2AN	139.2(2)	143.7(2)	142.5(2)	137.0(2)	143.9(2)	135.5(2)	143.1(2)
1,7-Ac_2AN	139.0(2)	142.8(2)	143.3(2)	135.6(2)	142.8(2)	137.4(1)	142.7(1)
1,8-Ac_2AN	139.2(2)	143.7(2)	142.8(2)	135.5(2)	141.4(3)	137.3(2)	144.4(2)
1,8-Ac_2AN	139.2(2)	143.7(2)	142.9(2)	135.2(3)	141.2(3)	137.5(2)	144.9(2)
2,7-Ac_2AN	139.4(3)	144.3(3)	142.3(3)	134.9(3)	142.8(3)	136.6(3)	141.8(3)
9,10-Ac_2AN	139.4(3)	143.8(3)	143.3(3)	135.2(4)	141.1(4)	136.5(4)	143.0(3)
	C^{8a}–C^9	C^9–C^{9a}	C^{9a}–C^1	C_{ar}–C^{11}	C^{11}–C^{12}	C^{11}-O	
AN[a]	140.1	140.1	143.4	–	–	–	
1-AcAN[b]	139.0(3)	138.9(3)	144.8(3)	149.3(3)	148.8(3)	121.7(3)	
2-AcAN	139.3(4)	139.7(4)	142.3(4)	148.6(4)	149.5(4)	121.5(3)	
9-AcAN[c]	140.3(3)	140.2(3)	142.4(3)	150.3(3)	148.5(3)	120.8(2)	
1,5-Ac_2AN	139.9(2)	139.7(2)	145.0(2)	149.4(2)	150.9(2)	121.8(2)	
1,6-Ac_2AN	139.5(2)	140.0(2)	144.6(2)	150.1(2)	150.5(2)	121.7(2)	
				149.3(2)	150.6(2)	121.8(2)	
1,7-Ac_2AN	140.5(1)	140.1(1)	145.5(1)	149.8(2)	151.6(2)	121.7(1)	
				149.0(2)	150.1(2)	122.1(1)	
1,8-Ac_2AN	140.1(2)	140.1(2)	144.4(2)	149.3(2)	151.2(2)	121.5(2)	
1,8-Ac_2AN	139.9(2)	139.9(2)	144.9(2)	148.9(2)	151.4(2)	121.4(2)	
2,7-Ac_2AN	139.3(3)	139.6(3)	141.9(3)	149.0(4)	150.0(4)	122.1(3)	
				148.9(3)	149.5(3)	121.0(3)	
9,10-Ac_2AN	140.0(3)	140.1(3)	142.9(3)	151.4(3)	149.4(3)	121.3(3)	
				151.5(3)	149.4(4)	120.0(3)	

[a] Brock & Dunitz, 1990; averaged bonds lengths
[b] Langer & Becker, 1993
[c] Zouev et al., 2011

Table 3. Bond lengths (pm) in the X-ray structures of anthracene, monoacetylanthracenes and diacetylanthracenes.

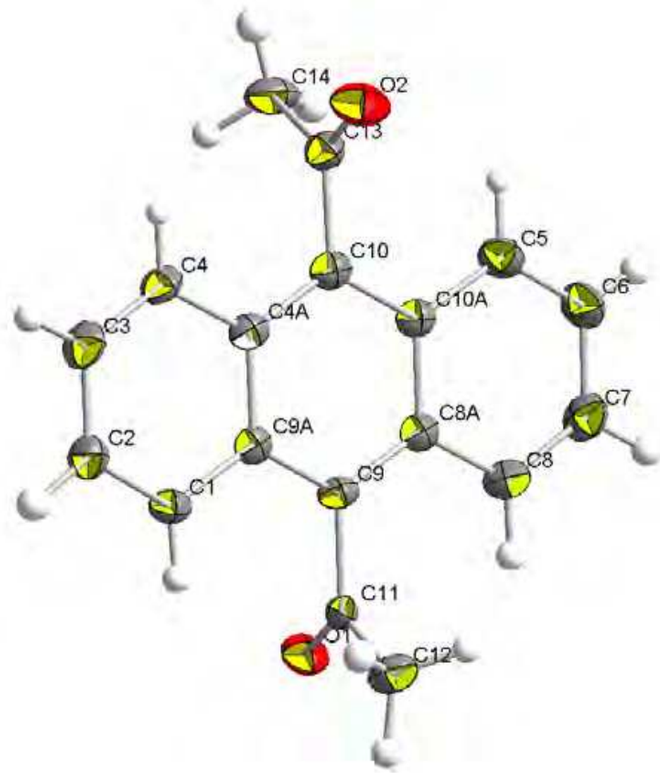

Fig. 10. ORTEP drawings of the crystal structure of 9,10-Ac_2AN, scaled to enclose 50% probability

Ketone 2-AcAN crystallizes in the *E* conformation with a small twist angle of $\tau_2(C^1–C^2–C^{11}–O^{13})$=173.1° and a small dihedral angle θ=5.9°. There are two pairs of enantiomeric molecules in the unit cell of 2-AcAN. The structure does not contain any short contact distances. Ketone 1,5-Ac_2AN adopts the *Z*,*Z* conformation with large twist angles, $\tau_1(C^{9a}–C^1–C^{11}–O^{15})$=20.0°, $\tau_1(C^{10a}–C^5–C^{13}–O^{16})$=–20.0°. The $O^{15}\cdots H^9$ and $O^{16}\cdots H^{10}$ contact distances are 226.9 pm, which is slightly shorter (7% penetration) than the sum of the respective van der Waals radii of hydrogen (115 ppm) and oxygen (129ppm) [Zefirov, 1997]. There are two identical molecules of 1,5-Ac_2AN in the unit cell, each posessing the C_i symmetry. Ketone 1,6-Ac_2AN crystallizes in the *Z*,*E* conformations, with a large twist angle of the *Z* carbonyl group, $\tau_1(C^{9a}–C^1–C^{11}–O^{15})$=30.0° and a small twist of the *E* carbonyl group, $\tau_2(C^5–C^6–C^{13}–O^{16})$=178.6°. The $O^{15}\cdots H^9$ contact distance is 228.8 pm (6% penetration), while the $O^{16}\cdots H^7$ contact distance is 249.9 pm. There are two enantiomeric molecules in the unit cell of 1,6-Ac_2AN. Ketone 1,7-Ac_2AN also crystallizes in the *Z*,*E* conformations, with the twist angles of $\tau_1(C^{9a}–C^1–C^{11}–O^{15})$=–15.2° and $\tau_2(C^8–C^7–C^{13}–O^{16})$=–176.6°. The $O^{15}\cdots H^9$ contact distance is 221.3 pm (9% penetration). There are two enantiomeric molecules in the unit cell of 1,7-Ac_2AN. Ketone 1,8-Ac_2AN adopts the *Z*,*Z* conformation with two large twist angles, due to the repulsive *peri*-interactions $O^{15}\cdots H^9$ and $O^{16}\cdots H^9$ (225.9 and 228.2 pm) between two carbonyl oxygens and the same aromatic hydrogen. There are two enantiomeric pairs of non-equivalent molecules, A and B, in the unit cell of 1,8-Ac_2AN, each of them posessing the C_2 symmetry. The respective twist angles are $\tau_1(C^{9a}–C^1–C^{11}–O^{15})$=–34.0° (A) and $\tau_1(C^{9a}–C^1–C^{11}–O^{15})$=–32.4° (B). Ketone 2,7-$Ac_2AN$ adopts the *E*,*Z* conformation, which is similar to

those of 1,6-Ac_2AN and 1,7-Ac_2AN but with a larger twist of the *E*-acetyl group, $\tau_2(C^1–C^2–C^{11}–O^{15})$=171.9°, and a smaller twist of the *Z*-acetyl group, $\tau_2(C^6–C^7–C^{12}–O^{16})$=0.9°. There are four pairs of enantiomeric molecules in the unit cell of 2,7-Ac_2AN. Ketone 9,10-Ac_2AN crystallizes in the *E* conformation with the twist angles of $\tau_9(C^{9a}–C^9–C^{11}–O^{15})$=–85.0° and $\tau_9(C^{10a}–C^{10}–C^{13}–O^{16})$=87.0°. There are two pairs of enantiomeric molecules in the unit cell of 9,10-Ac_2AN. According to the literature structure [Langer & Becker, 1993], 1-AcAN crystallizes in the *Z*-conformation with a twist angle of $\tau_1(C^{9a}–C^1–C^{11}–O^{13})$=27.1°. The carbonyl group of ketone 9-AcAN [Zouev2011] is nearly orthogonal to the aromatic plane, $\tau_9(C^1–C^2–C^{11}–O^{13})$=87.9°.

None of the mono- and diacetylanthracenes under study adopts a planar conformation in their crystal structures. The absolute values of the twist angles in the mono- and diacetylanthracenes vary, depending on the position of substitution and on the conformation of the acetyl groups: $|\tau_1|$=15.2–34.0° for the 1*Z*-acetyl groups, $|\tau_2|$=0.9° for the 2*Z*-acetyl group, $|\tau_2|$=171.9–178.6° for the 2*E*-acetyl groups, and $|\tau_9|$=85.0–87.9°. The higher twist angles of the 1*Z*-acetyl groups are caused by the repulsive interactions between the carbonyl oxygen and the respective *peri*-hydrogen. The acetyl groups themselves are nealry planar (excluding the methyl hydrogens), and the pyramidalization angles χ at the carbonyl carbon atom are small, 0.1–3.4°. The dihedral angles θ between the plane of the carbonyl group and the aromatic plane are very close to the respective twist angles τ (Table 2). The anthracene systems in the mono- and diacetylanthracenes under study are also essentially planar: the dihedral fold angles φ between the side six-membered rings of the anthracene unit are 0.0–5.8°. The pyramidalization angles χ at the carbon atom bonded to the acetyl substituent are small, 0.1–4.7°. Thus, the twist of the acetyl group(s) is the main feature of non-planarity in the mono- and diacetylanthracenes.

The diacetylanthracenes under study can be arranged in the order of decreasing twist angles τ:

9,10-Ac_2AN>>1,8-Ac_2AN>1,6-Ac_2AN>1,5-Ac_2AN>1,7-Ac_2AN>2,7-Ac_2AN.

The magnitude ot the twist angle of the acetyl group is important. It has been shown that if an acyl group is tilted out of the plane of the aromatic ring of an aromatic ketone by neighboring bulky groups, the resonance stabilization is reduced and the pattern irreversibility of Friedel–Crafts acylation may be challenged, allowing deacylation, transacylation and acyl rearrangments [Buehler & Pearson, 1970; Gore, 1974; Mala'bi, et al., 2011]. Thus, the twist angle τ may define the ability of diacetylanthracenes to undergo deacylations and rearrangements according to Agranat-Gore rearrangement.

Another factor that may influence the tilting of the acetyl group and, as a consequence, the feasibility of acyl rearrangements, is the overcrowding. Its main source is the short contact distances between the carbonyl oxygen and the *peri*-hydrogen, or between the methyl group and *peri*-hydrogen. The intramolecular O···H distances in the crystal structures of the mono- and diacetylanthracenes under study are not particularly short, 221–246 pm, for the *Z*-acetyl groups, which corresponds to 0–9% penetration. There are no close contact distances caused by the *E*-acetyl groups.

2.1.2 Intermolecular interactions in monoacetylanthracenes and diacetylanthracenes

Aromatic–aromatic interactions are non-covalent intermolecular forces similar to hydrogen bonding [Janiak, 2000]. Aromatic systems may be arranged in three principal configurations:

- A stacked (**S**) configuration, or a π···π interaction, in which aromatic rings are face-to-face aligned, with the interplanar distances of about 3.3–3.8 Å [Janiak, 2000]. This configuration has the maximal overlap but it is rarely observed in real systems containing aromatic rings [Sinnokrot & Sherrill, 2006].
- The T-shaped configuration (**T**), or a C–H···π interaction, where one aromatic ring points at the center of another ring.
- The parallel displaced (**D**), or offset stacked, configuration; it is reached from the stacked configuration by the parallel shift of one aromatic ring relative to the other [Sinnokrot & Sherrill, 2006], and features both π-π and C–H···π interactions. The **T**- and **D**-type configurations are often observed in small aromatic compounds [Dahl, 1994] and proteins [Hunter et al., 1991].

The crystal structure of the parent anthracene (AN) has been studied [Brock & Dunitz, 1990; Sinclair et al., 1950; Murugan & Jha, 2009]. It crystallizes in the monoclinic space group $P2_1/a$. Within the unit cell, the anthracene molecules are packed in a "herringbone" pattern, similar to the parent PAH naphthalene [Desiraju & Gavezzotti, 1989]. In this motif, the C···C non-bonded interactions are between non-parallel nearest neighbor molecules. The herringbone packing is one of four basic structural types for PAH, which are defined depending on the shortest cell axis and the interplanar angle [Desiraju & Gavezzotti, 1989]. The structures with herringbone packing, "sandwich herringbone" packing and γ packing obtain crystal stabilization mainly from C···C interactions, but also from C···H interactions [Desiraju & Gavezzotti, 1989]. The "graphitic", or β, packing characterized by strong C···C interactions without much contribution from C···H contacts [Desiraju & Gavezzotti, 1989]. The selected geometric parameters of aromatic interactions in the mono- and diacetylanthracenes under study are presented in Table 4. *Cg*1 is the centroid for the C^1–C^2–C^3–C^4–C^{4a}–C^{9a} ring, *Cg*2 is the centroid for the C^{4a}–C^{10}–C^{10a}–C^{8a}–C^9–C^{9a} ring and *Cg*3 is the centroid for the C^5–C^6–C^7–C^8–C^{8a}–C^{10a} ring; *Cg*4–6 are the respective centroids of the second non-equivalent molecule in the unit cell, if it exists. Interplanar angle is the angle between the planes of adjacent molecules. Slippage distance is distance of one centroid from the projection of another centroid. Displacement angle is the angle between the ring normal and the centroid vector.

The molecules of 2-AcAN are packed in a "herringbone" pattern, with the interplanar angle of 51.0°. The anthracene moieties in the crystal structure of 2-AcAN adopt the **T**-configuration with the shortest centroid-centroid separation of 464.7 pm. The shortest distances between the centroids of one molecule and the carbon atoms of the other molecule are *Cg*3'···C^4=343.7 pm, *Cg*2'···C^8=351.2 pm, *Cg*2'···C^{10}=351.2 pm, *Cg*3'···C^9=357.6 pm and *Cg*1'···C^5=358.2 pm. The respective centroid–hydrogen distances are *Cg*3'···H^4=271.5 pm, *Cg*2'···H^8=283.3 pm, *Cg*2'···H^{10}=280.8 pm, *Cg*3'···H^9=288.2 pm and *Cg*1'···H^5=287.9 pm. The π···π interactions in 2-AcAN are very weak despite close lying parallel planes, as reflected in very long distances between the respective centroids (>584 pm). Thus, the aryl C–H···π interactions dominate in the crystal structure of 2-AcAN. The unit cell of 2-AcAN is shown in Figure 11.

The molecules of 1,5-Ac_2AN are packed in a "herringbone" pattern, with the interplanar angle of 56.2°. The anthracene moieties in the crystal structure of 1,5-Ac_2AN adopt the **T**-configuration with the shortest centroid-centroid separation of 462.9 and 470.5 pm. The shortest distances between the centroids of one molecule and the carbon atoms of the other molecule are *Cg*1'···C^4=341.9 pm, *Cg*1'···C^3=353.6 pm and *Cg*2'···C^4=376.3 pm. The respective centroid–hydrogen distances are *Cg*1'···H^4=264.3 pm, *Cg*1'···H^3=293.7 pm and *Cg*2'···H^4=342.9 pm. Thus, the aryl C–H···π interactions dominate in the crystal structure of 1,5-Ac_2AN, while

the π···π interactions are not possible due to very long distances between molecules lying in the parallel planes (>600 pm). The unit cell of 1,5-Ac_2AN is shown in Figure 12.

Fig. 11. The unit cell of 2-AcAN (view along *c* axis)

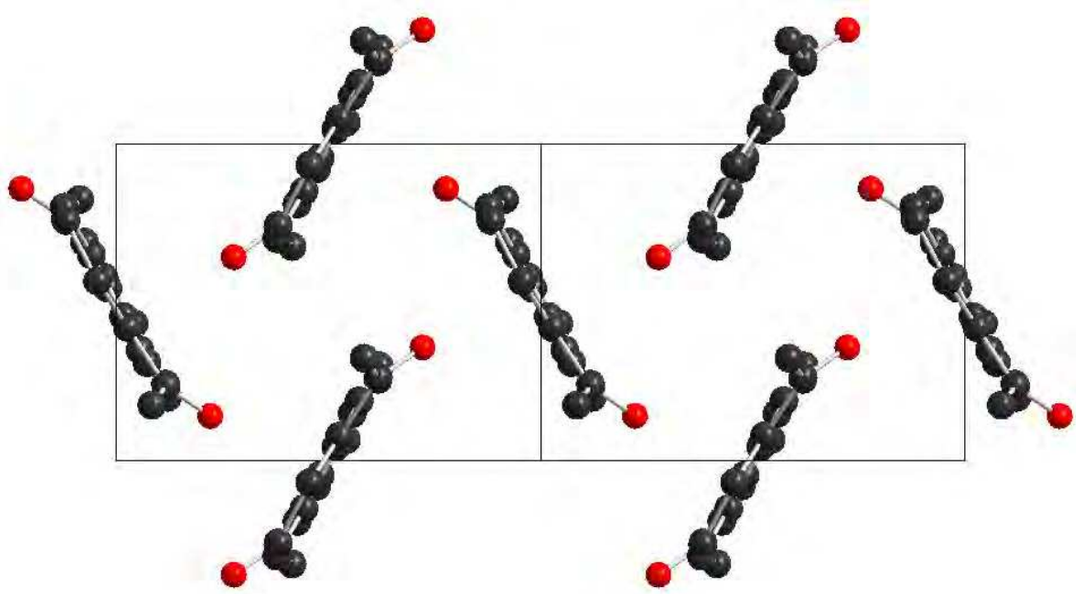

Fig. 12. The unit cell of 1,5-Ac_2AN (view along special axis *1,0,1*)

The molecules of 1,6-Ac_2AN are packed by β type, forming a layered structure made up of "graphitic" planes with zero interplanar angle. From the point of view of aromatic–aromatic interactions, the anthracene moieties in the crystal structure of 1,6-Ac_2AN are stacked by the **D**-type, with the centroid–centroid separation of 359.2 and 385.6 pm. The slippage distances

of the centroids are relatively short, 94.0 and 107.1 pm. The shortest contact distances between the aromatic carbons in 1,6-Ac_2AN are $C^{5\cdots}C^{7'}$=355.1 and $C^{6\cdots}C^{8a'}$=358.5. The unit cell of 1,6-Ac_2AN is shown in Figure 13.

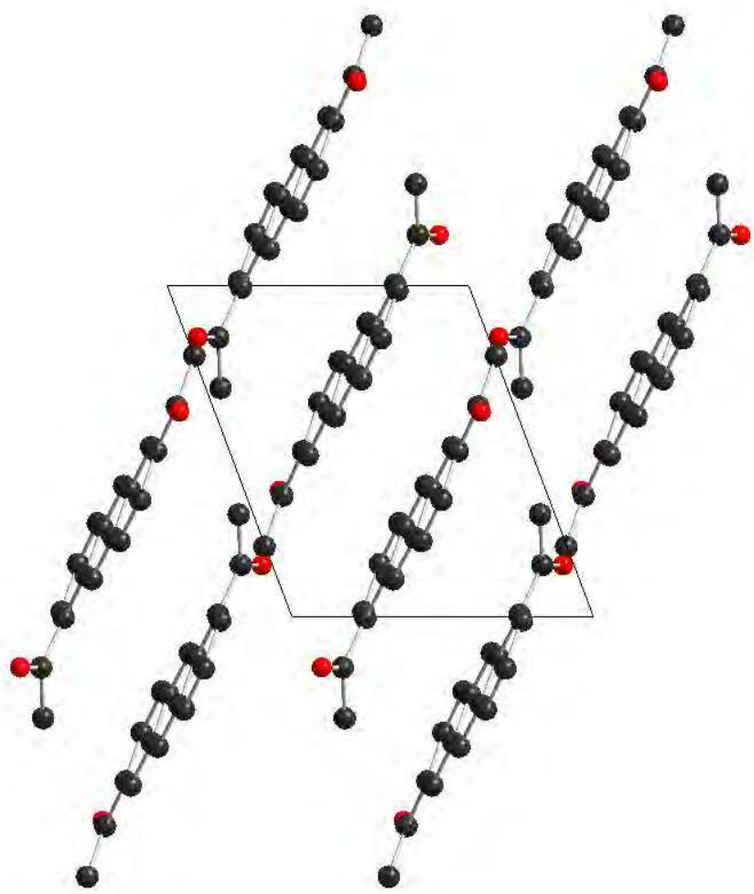

Fig. 13. The unit cell of 1,6-Ac_2AN (view along *c* axis)

The molecules of 1,7-Ac_2AN are also packed by β type. The anthracene moieties in the crystal structure of 1,7-Ac_2AN adopt the **D**-configuration, with the shortest centroid-centroid separation of 370 pm. Despite the longer slippage distance between centroids (154.4–154.8 pm), the contact distances in 1,7-Ac_2AN are shorter than those in 1,6-Ac_2AN: $C^{3\cdots}C^{8'}$=333.3, $C^{4a\cdots}C^{9'}$=336.4, $C^{8\cdots}C^{9'}$=337.1 and $C^{1\cdots}C^{10'}$=340.9. In both 1,6-Ac_2AN and 1,7-Ac_2AN the aromatic interactions are mainly those of the π··π type. The unit cell of 1,7-Ac_2AN is shown in Figure 14.

The molecules of 1,8-Ac_2AN are packed in a "herringbone" pattern, with the interplanar angle of 34.7°. The centroids of the anthracene molecules lying onto the parallel planes are separated by 580–581 pm. These distances together with the slippage distance of 493-494 pm render the aromatic interactions of either **S**- or **D**-type impossible. The **T**-type interactions in 1,8-Ac_2AN are too weak to be of any importance, due to the long distances between centroids (546–562 pm). However, the plane of the acetyl group (containing C^1, C^{11}, C^{13}, O^{15}) of molecule A forms the angle of 4.0° with the aromatic plane of molecule B. Analogously,

the plane of the acetyl group (containing $C^{1'}$, $C^{11'}$, $C^{13'}$, $O^{15'}$) of molecule B is nearly parallel to the aromatic plane of molecule A, 3.8°. The distances between the anthracene systems and the carbonyl group are sufficiently small to consider the intermolecular π···π interactions: $Cg4'\cdots O^{1}$=353.8 pm, $Cg4'\cdots C^{11}$=384.3 pm, $Cg3\cdots O^{1'}$=363.3 pm and $Cg3\cdots C^{11'}$=398.2 pm. Thus, the crystal structure of 1,8-Ac_2AN features π–π-interactions not between two aromatic systems, but between the aromatic system and the carbonyl π-bond. The unit cell of 1,8-Ac_2AN is shown in Figure 15.

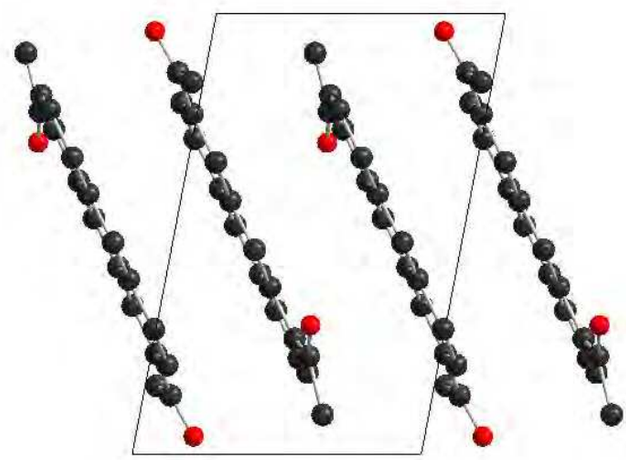

Fig. 14. The unit cell of 1,7-Ac_2AN (view along *b* axis)

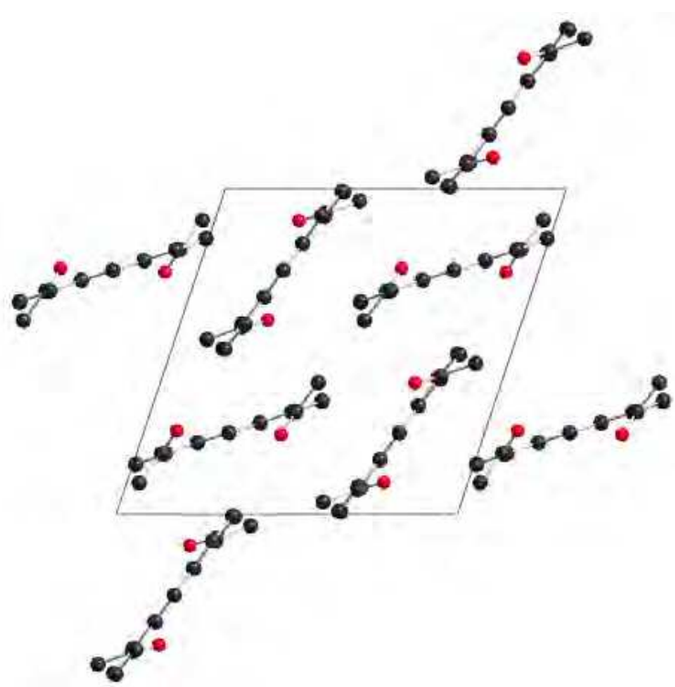

Fig. 15. The unit cell of 1,8-Ac_2AN (view along *b* axis)

The molecules of 2,7-Ac_2AN are packed in a "herringbone" pattern. The anthracene moieties in the crystal structure of 2,7-Ac_2AN adopt the **T**-configuration, similarly to 1,5-Ac_2AN. The planes of the adjacent molecules form the angle of 58.1°. The shortest distances between the centroids and the carbon atoms are $Cg3\cdots C^4$=358.4 pm and $Cg1\cdots C^5$=375.5 pm on the one side of the anthracene system, and $Cg3\cdots C^9$=374.0 pm, $Cg2\cdots C^8$=374.8 pm on the other side. The respective shortest centroid–aryl hydrogen distances are $Cg1\cdots H^5$=299.3 pm and $Cg3\cdots H^4$=283.5 pm. The **D**-type interactions in 2,7-Ac_2AN are very weak due to the large separation of centroids (420–433 pm) and large slippage distances (226–242 pm). The unit cell of 2,7-Ac_2AN is shown in Figure 16.

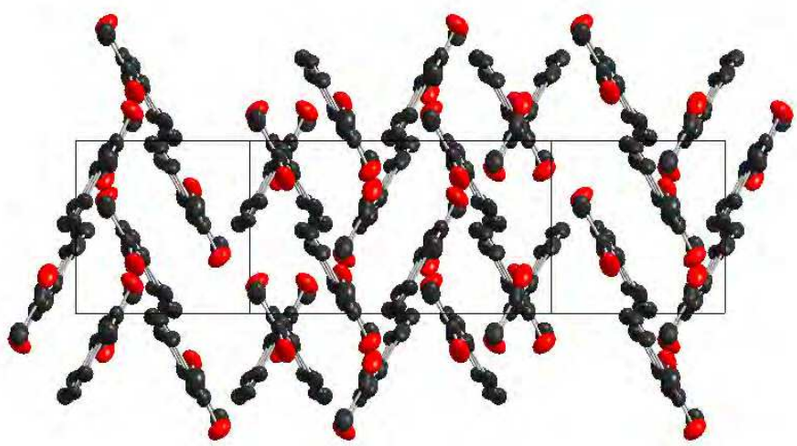

Fig. 16. The unit cell of 2,7-Ac_2AN (view towards plane *1,0,–5*)

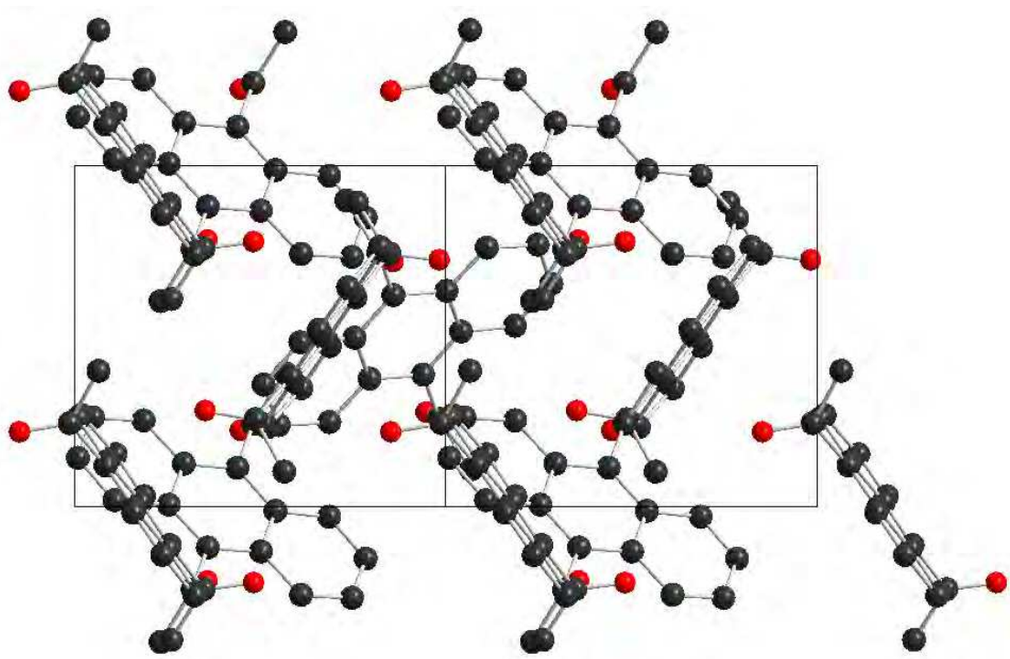

Fig. 17. The unit cell of 9,10-Ac_2AN (view along special axis *1,0,1*)

The anthracene moieties in the crystal structure of 9,10-Ac_2AN adopt the **T**-configuration, similarly to 1,5-Ac_2AN and 2,7-Ac_2AN. The planes of the adjacent molecules form the angle of 73.6°. The shortest distances between the centroids and the carbon atoms are *Cg*2···C^7=356.1 pm, *Cg*2···C^8=379.6 pm and *Cg*1···C^8=384.7 pm. The respective shortest centroid–aryl hydrogen distances are *Cg*2···H^7=287.9 pm, *Cg*2···H^8=329.4 pm and *Cg*1···H^8=294.4 pm. The **D**-type interactions in 9,10-Ac_2AN are non-existent. The molecules lying in the parallel planes are separated by >720 pm, probably due to the considerable twist angles of the acetyl group in 9,10-Ac_2AN (–85.0° and 87.0°), making the tighter arrangement impossible. The unit cell of 9,10-Ac_2AN is shown in Figure 17.

	Centroid	Centroid	Centroid centroid distance pm	Interplanar distance pm	Interplanar angle deg	Slippage distance pm	Displacement angle deg
2-AcAN	*Cg*1	*Cg*3'[a]	464.7	–	51.0	110.8	13.8
	*Cg*1	*Cg*3'[b]	477.2	–	51.0	103.6	12.5
	*Cg*1	*Cg*3'[c]	499.5	–	51.0	209.7	24.8
	*Cg*1	*Cg*3'[d]	511.1	–	51.0	205.9	23.8
	*Cg*1	*Cg*2'[e]	584.5	251.6	0.0	544.4	64.5
1,5-Ac_2AN	*Cg*2	*Cg*1'[f]	462.9	–	56.2		
	*Cg*1	*Cg*1'[g]	470.5	–	56.2		
	*Cg*2	*Cg*1'[h]	601.5	292.2	0.0	526.4	61.1
	*Cg*3	*Cg*2'[h]	601.5	292.2	0.0	525.8	60.9
1,6-Ac_2AN	*Cg*3	*Cg*3'[i]	359.2	346.1	0.0	94.0	15.2
	*Cg*1	*Cg*1'[j]	385.6	370.4	0.0	107.1	16.1
1,7-Ac_2AN	*Cg*1	*Cg*3'[i]	370.1	335.9	0.0	154.6	24.7
	*Cg*1	*Cg*2'[i]	370.4	335.9	0.0	154.8	24.7
	*Cg*2	*Cg*2'[i]	370.2	335.9	0.0	154.4	24.7
1,8-Ac_2AN	*Cg*1	*Cg*4'[k]	546.4	–	34.7		
	*Cg*1	*Cg*4'[l]	561.5	–	34.7		
	*Cg*1	*Cg*1'[i]	580.5	307.2	0.0	492.6	58.1
	*Cg*1	*Cg*1'[m]	580.9	305.9	0.0	493.9	58.2
2,7-Ac_2AN	*Cg*2	*Cg*3'[n]	419.8	354.6	0.0	226.2	32.6
	*Cg*3	*Cg*3'[n]	432.7	354.6	0.0	241.8	35.2
	*Cg*1	*Cg*3'[o]	481.0	–	58.1		
	*Cg*2	*Cg*2'[o]	486.6	–	58.1		
9,10-Ac_2AN	*Cg*2	*Cg*3'[p]	475.5	–	73.6		
	*Cg*2	*Cg*1'[q]	481.8	–	73.6		
	*Cg*3	*Cg*2'[r]	721.2	478.0	0.0	540.1	48.5
	*Cg*2	*Cg*1'[r]	722.3	478.0	0.0	541.5	48.6
	*Cg*3	*Cg*1'[r]	724.2	478.0	0.0	544.0	48.7

Symmetry codes: [a] 0.5–*x*, 0.5+*y*, 1.5–*z*; [b] 0.5–*x*, –0.5+*y*, 1.5–*z*; [c] 1.5–*x*, 0.5+*y*, 1.5–*z*; [d] 1.5–*x*, –0.5+*y*, 1.5–*z*; [e] –1+*x*, *y*, *z*; [f] *x*, 0.5–*y*, 0.5–*z*; [g] 1–*x*, 0.5+*y*, 0.5–*z*; [h] *x*, 1+*y*, *z*; [i] 1–*x*, 1–*y*, 1–*z*; [j] 1–*x*, –*y*, –*z*; [k] 1.5–*x*, 1+*y*, 1.5–*z*; [l] 1–*x*, –*y*, 1–*z*; [m] 0.5+*x*, –*y*, –0.5+*z*; [n] 0.5–*x*, 0.5–*y*, 0.5–*z*; [o] –x, 0.5+*y*, 0.5–*z*; [p] –0.5+*x*, 1.5–*y*, *z*; [q] 0.5+*x*, 0.5–*y*, *z*; [r] *x*, –1+*y*, *z*.

Table 4. Aromatic interactions in monoacetylanthracenes and diacetylanthracenes

Thus, the monoacetylanthracenes and diacetylanthracenes under study may be divided into two groups, based on the aromatic–aromatic interactions in their crystal structures. The anthracene units in 1,6-Ac_2AN and 1,7-Ac_2AN are offset stacked (the **D**-type arrangement) and feature aromatic–aromatic π···π interactions. The anthracene molecules in ketones 2-AcAN, 1,5-Ac_2AN, 2,7-Ac_2AN and 9,10-Ac_2AN adopt the **T**-type arrangement, and feature aryl C–H···π interactions. The analysis of the literature crystal structures of 1-AcAN and 9-AcAN shows that these ketones also adopt the **T**-type arrangement. In 1-AcAN, 9-AcAN, 1,5-Ac_2AN and 9,10-Ac_2AN the considerable twist angles of the acetyl groups prevents the molecules from being arranged in close lying parallel planes. The exception is the crystal structure of 1,8-Ac_2AN, which features π···π-interactions between the aromatic system and the carbonyl π-bond. Most likely the methyl groups are the reason for the lack of more examples of slipped-stacking and also in some cases the competing ketone–π system as well. It should be noted, however, that the centroid–centroid analysis can be misleading, and its limitations should not be overlooked.

Another kind of intermolecular interactions that could exist in acetylanthracenes is hydrogen bonds. No particular strong intermolecular aryl C–H···O bonds have been found in the diacetylanthracenes under study. The shortest contact distances between an oxygen and an aromatic hydrogen are $O^{15}\cdots H^{5}$=242.2 pm (9,10-Ac_2AN), $O^{15}\cdots H^{1}$=247.4 pm and $O^{16}\cdots H^{9}$=259.4 pm (2,7-Ac_2AN), $O^{15}\cdots H^{5}$=255.6 pm (1,6-Ac_2AN), $O^{16}\cdots H^{3}$=256.4 pm and $O^{15}\cdots H^{4}$=260.7 pm (1,7-Ac_2AN), $O^{15}\cdots H^{2'}$=260.5 pm (1,8-Ac_2AN), $O^{15}\cdots H^{2}$=284.6 pm (1,5-Ac_2AN). The shortest contact distances between an oxygen and a methyl hydrogen are of a similar magnitude: $O^{15}\cdots H^{14c}$=240.8 pm (2,7-Ac_2AN), $O^{16}\cdots H^{12c}$=254.7 pm (1,6-Ac_2AN), $O^{16}\cdots H^{12b}$=257.5 pm (1,7-Ac_2AN), $O^{15}\cdots H^{12c}$=259.4 pm (1,5-Ac_2AN), $O^{15}\cdots H^{12c}$=265.9 pm (9,10-Ac_2AN).

2.2 NMR Study of monoacetylanthracenes and diacetylanthracenes

The structure of a compound in crystal is not necessarily the same as that in solution. More often, in the case of substances that are not conformationally homogeneous, e.g. diacetylanthracenes, the crystal has a unique conformation and the conformational heterogeneity appears in fluid phases [Eliel & Wilen, 1994]. An insight into the conformations of mono- and diacetylanthracenes in solution may be gained from the chemical shifts of the aromatic protons adjacent to the carbonyl groups. The magnetic shielding (or deshielding) effect on the chemical shifts of protons that lie in or near the plane of the carbonyl group is well known. The McConnell equation [McConnel, 1957] predicts shielding for protons lying above the center of a carbon–oxygen double bond and deshielding for protons located within a cone aligned with the carbon–oxygen bond axis. The McConnell model, however, takes into account only the effect of magnetic anisotropy.

Recently, more detailed shielding model has been proposed [Martin et al., 2003]. According to this model, shielding is predicted for protons located in the region from over the center of the carbon–oxygen double bond to beyond the carbon atom; deshielding is predicted for protons located above and beyond the oxygen atom. Table 5 gives ^{1}H-NMR chemical shifts for the monoacetylanthracenes and diacetylanthracenes under study, together with the chemical shifts in parent anthracene (AN).

The data presented in Table 5 show that the protons at *ortho*-positions to an acetyl group are considerably deshielded as compared with the protons of unsubstituted anthracene. The magnitudes of the low field shifts of the *ortho*-protons are similar among

monoacetylanthracenes and diacetylanthracenes: Δδ(H^1, ppm)=0.70 (2-AcAN), 0.72 (2,7-Ac_2AN); Δδ(H^2, ppm)=0.59 (1-AcAN), 0.63 (1,6-Ac_2AN), 0.67 (1,5-Ac_2AN), 0.67 (1,7-Ac_2AN), 0.73 (1,8-Ac_2AN); Δδ(H^3, ppm)=0.61 (2-AcAN), 0.65 (2,7-Ac_2AN); Δδ(H^5, ppm)=0.62 (1,6-Ac_2AN); Δδ(H^6, ppm)=0.63 (1,7-Ac_2AN), 0.65 (2,7-Ac_2AN), 0.67 (1,5-Ac_2AN); Δδ(H^7, ppm)=0.58 (1,6-Ac_2AN), 0.73 (1,8-Ac_2AN); Δδ(H^8, ppm)=0.72 (2,7-Ac_2AN), 0.77 (1,7-Ac_2AN). The protons at *peri*-positions to an acetyl group are deshielded with even greater magnitudes: Δδ(H^9, ppm)=1.06 (1,6-Ac_2AN), 1.08 (1-AcAN), 1.17 (1,5-Ac_2AN), 1.27 (1,7-Ac_2AN), 1.78 (1,8-Ac_2AN). The latter case is special because of the presence of two acetyl groups at *peri*-positions to H^9, which nearly double its low field chemical shift. Note that in 2-AcAN, 1,6-Ac_2AN, 1,7-Ac_2AN and 2,7-Ac_2AN both protons *ortho* to the acetyl groups demonstrate similar low field shifts, suggesting that these protons are located above the plane of the carbonyl group and near the oxygen atom [Martin et al., 2003]. Thus, the twist angles of the acetyl groups of mono- and diacetylanthracenes are small, in accordance with their respective X-ray crystal structures, and *E*,*Z*-diastereomerizations of the acetyl groups at both α (1, 5, 8) and β (2, 6, 7) positions are swift on the NMR time scale.

	H^1	H^2	H^3	H^4	H^5	H^6	H^7	H^8	H^9	H^{10}	CH_3	CH_3
AN	7.95	7.41	7.41	7.95	7.95	7.41	7.41	7.95	8.40	8.40		
1-AcAN		7.998	7.469	8.169	7.998	7.528–7.495	7.528–7.495	8.083	9.482	8.446	2.810	
2-AcAN	8.646		8.054–7.982	8.054–7.982	8.054–7.984	7.546	7.516	8.054–7.984	8.573	8.432	2.763	
9-AcAN	7.859	7.556–7.477	7.556–7.477	8.027	8.027	7.556–7.477	7.556–7.477	7.859		8.473	2.822	
1,5-Ac_2AN		8.083	7.530	8.262		8.083	7.530	8.262	9.570	9.570	2.818	2.818
1,6-Ac_2AN		8.040	7.490	8.153	8.570		7.994	8.064	9.457	8.523	2.796	2.730
1,7-Ac_2AN		8.080	7.559	8.199	8.036	8.036		8.719	9.673	8.460	2.836	2.773
1,8-Ac_2AN		8.140	7.514	7.964	7.964	7.514	8.140		10.175	8.471	2.840	2.840
2,7-Ac_2AN	8.670		8.063	8.063	8.063	8.063		8.670	8.718	8.449	2.775	2.775
9,10-Ac_2AN	7.881–7.845	7.571–7.537	7.571–7.537	7.881–7.845	7.881–7.845	7.571–7.537	7.571–7.537	7.881–7.845			2.816	2.816

Table 5. The ^{1}H-NMR chemical shifts (δ, ppm) of aromatic and methyl protons in anthracene (AN), monoacetylanthracenes and diacetylanthracenes under study.

Ketones 9-AcAN and 9,10-Ac_2AN differ from the rest of the mono- and diacetylanthracenes. The protons at *peri*-positions to the acetyl groups of 9-AcAN and 9,10-Ac_2AN are slightly shielded: Δδ(H^1, ppm)= –0.09 (9-AcAN), –0.09 (9,10-Ac_2AN). This suggests that the carbonyl groups in 9-AcAN and 9,10-Ac_2AN are turned away of the protons at *peri*-positions, and these protons are located near the carbonyl carbon atoms, which implies high twist angles of the acetyl groups. It corresponds well to the respective X-ray crystal structures of 9-AcAN and 9,10-Ac_2AN.

2.3 DFT computational study of monoacetylanthracenes and diacetylanthracenes

DFT methods are capable of generating a variety of isolated molecular properties quite accurately, especially via the hybrid functional, and in a cost-effective way [deProft & Geerlings, 2001, Koch & Holthausen, 2000]. The B3LYP hybrid functional was successfully employed to treat overcrowded BAEs [Biedermann et al., 2001, Pogodin et al., 2006] and overcrowded naphthologues of BAEs-1, i.e. mono-bridged tetraarylethylenes [Assadi et al., 2009]. The monoacetylanthracenes and diacetylanthracenes under study were subjected to a systematic computational DFT study of their conformational spaces and of their relative stabilities. The B3LYP/6-31G(d) relative energies of the global minima conformations of certain diacetylanthracenes have been previously reported [Mala'bi et al., 2011]. The total and relative B3LYP/6-31G(d) energies (E_{Tot} and ΔE_{Tot}) and Gibbs free energies (ΔG_{298} and $\Delta\Delta G_{298}$) of the acetylanthracenes are presented in Table 6. Selected calculated geometrical parameters of the acetylanthracenes are also given in Table 6. The following geometrical parameters were considered: the twist angles τ_1, τ_2 and τ_9 and the respective twist angles υ around the anthracenyl–carbonyl bond; the dihedral angle θ between the least-square planes of the carbonyl group and the anthracene system; the dihedral angle φ between the least-square planes of two side rings of the anthracene system; the pyramidalization angles χ at C^1, C^2 and C^9.

2.3.1 Conformational space of monoacetylanthracenes and diacetylanthracenes

Monoacetylanthracenes may adopt two conformations, *Z* and *E*, defined by the twist angle of the carbonyl group. Diacetylanthracenes may adopt four conformations, i. e. *ZZ*, *ZE*, *EZ* and *EE*; in certain cases, *ZE* is identical to *EZ*. In addition, the oxygen atoms of two carbonyl groups may be located on the same side of the aromatic plane, or on the opposite sides, potentially resulting in *syn*- and *anti*-*ZZ*, *ZE*, *EZ* and *EE* conformations, respectively. Depending on the symmetry constraints and the twist angle τ, not all of the above-mentioned conformations exist for a given diacetylanthracene. The possible conformations of diacetylanthracene are shown in Fig. 18.

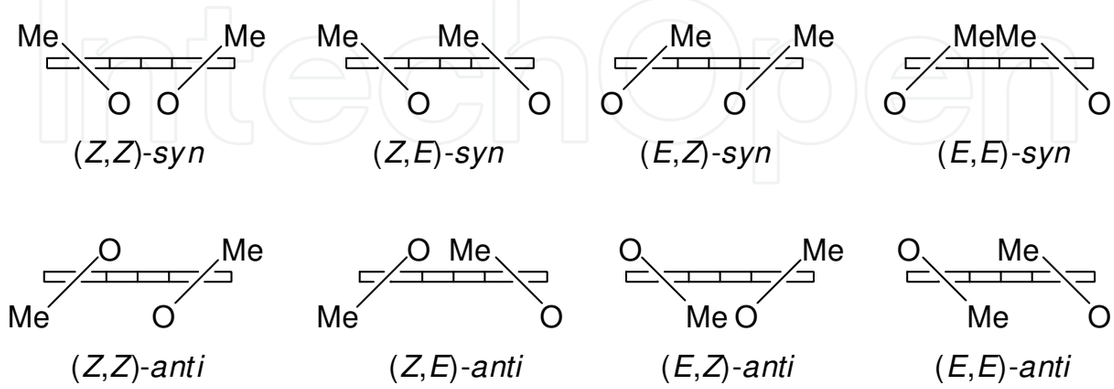

Fig. 18. Schematic representation of the eight possible conformations of a diacetylanthracene (view along the aromatic plane).

			E_{Tot}	ΔE_{Tot}	ΔG_{298}	$\Delta\Delta G_{298}$	τ[a]	υ[b]	θ	φ	C_{11}–C_{arom}[c]	χ
			Hartree	kJ/mol	kJ/mol	kJ/mol	deg	deg	deg	deg	pm	deg
1-AcAN	*Z*	C_s	–692.17301155	14.66	15.79	0.00	0.0	180.0	0.0	0.0	149.9	0.0
1-AcAN	[d] *Z*	C_1	–	–	–	–	27.1	–152.7	28.6	3.2	149.3	–0.1
1-AcAN	*E*	C_1	–692.16815672	27.41	28.80	13.01	150.8	–31.1	36.0	3.7	150.7	1.9
2-AcAN	*E*	C_s	–692.17859715	0.00	0.00	0.00	180.0	0.0	0.0	0.0	149.6	0.0
2-AcAN	[d] *E*		–	–	–	–	173.1	-5.3	5.9	0.4	149.6	–1.6
2-AcAN	*Z*	C_s	–692.17777414	2.16	2.24	2.24	0.0	180.0	0.0	0.0	149.9	0.0
9-AcAN	–	C_1	–692.16381815	38.80	36.94	0.00	–67.0	113.9	69.8	1.7	151.3	–1.0
9-AcAN	[d] –	C_1	–	–	–	–	87.9	–91.8	89.2	5.8	150.4	0.3
1,5-Ac_2AN	*ZZ*	C_{2h}	–844.81621983	24.25	27.69	0.00	0.0	180.0	0.0	0.0	149.8	0.0
1,5-Ac_2AN	[d] *ZZ*	C_i	–	–	–	–	20.0	–156.8	22.7	0.0	149.4	–3.2
1,5-Ac_2AN	*ZE*	C_1	–844.81074449	38.62	40.48	12.79	152.4	–29.3	34.1	3.8	150.6	1.6
							–1.1	178.9	2.3		150.0	0.0
1,5-Ac_2AN	*EEanti*	C_i	–844.80527143	52.99	55.06	27.36	150.6	–30.9	34.8	0.0	150.8	1.5
1,5-Ac_2AN	*EEsyn*	C_2	–844.80559961	52.13	55.74	28.05	151.9	–29.9	35.6	7.4	150.7	1.7
1,6-Ac_2AN	*ZE*	C_s	–844.82056764	12.83	13.45	0.00	0.0	180.0	0.0	0.0	150.0	0.0
							180.0	0.0	0.0		149.7	0.0
1,6-Ac_2AN	[d] *ZE*	C_1	–	–	–	–	30.0	–147.1	32.2		150.1	–2.9
							178.6	–0.7	1.9	1.3	149.3	–0.7
1,6-Ac_2AN	*ZZ*	C_s	–844.82005388	14.18	15.14	1.69	0.0	180.0	0.0	0.0	150.0	0.0
							0.0	180.0	0.0		150.0	0.0
1,6-Ac_2AN	*EE*	C_1	–844.81569542	25.63	27.03	13.57	150.6	–31.1	36.0	3.6	150.8	1.7
							179.9	–0.1	1.4		149.8	–0.1
1,6-Ac_2AN	*EZanti*	C_1	–844.81493981	27.61	28.88	15.43	150.6	–31.2	36.2		150.7	1.7
							–0.3	179.8	1.7		150.0	–0.1
1,7-Ac_2AN	*ZE*	C_s	–844.82110775	11.42	12.34	0.00	0.0	180.0	0.0	0.0	150.0	0.0
							180.0	0.0	0.0		149.7	0.0
1,7-Ac_2AN	[d] *ZE*	C_1	–	–	–	–	–15.2	162.9	16.0	2.3	149.8	1.9
							–176.6	3.7	4.5		149.0	0.3
1,7-Ac_2AN	*ZZ*	C_s	–844.81939574	15.91	15.83	3.50	0.0	180.0	0.0	0.0	150.1	0.0
							0.0	180.0	0.0		150.0	0.0
1,7-Ac_2AN	*EE*	C_1	–844.81562930	25.80	26.79	14.45	150.3	–31.4	36.3	3.7	150.8	1.7
							179.6	–0.5	1.7		149.8	0.0
1,7-Ac_2AN	*EZanti*	C_1	–844.81488173	27.76	28.96	16.62	150.8	–31.0	35.8	3.5	150.9	1.7
							0.2	–179.8	1.1		150.1	0.0
1,8-Ac_2AN	*ZZanti*	C_2	–844.81111292	37.66	38.89	0.00	–17.3	160.4	19.3	2.2	150.2	2.3
1,8-Ac_2AN	[d] *ZZ*	C_2	–	–	–	–	–34.0	145.4	36.0	0.3	149.3	0.6
							–32.4	144.9	35.4	3.4	148.9	2.7
1,8-Ac_2AN	*EZ*	C_1	–844.81126554	37.26	39.25	0.35	150.4	–31.2	36.1	3.5	151.1	1.6
							1.5	–178.3	2.6		150.0	0.2
1,8-Ac_2AN	*EEsyn*	C_s	–844.80423404	55.72	56.49	17.60	147.9	–33.8	40.2	7.0	150.7	1.7
1,8-Ac_2AN	*EEanti*	C_2	–844.80485619	54.08	56.56	17.66	148.1	–33.7	38.6	5.1	150.7	1.8
1,9-Ac_2AN	*ZZanti*	C_1	–844.79904569	69.34	70.32	0.00	–50.9	120.3	59.9	7.5	150.8	8.8
							–59.6	114.1	62.8		151.5	–6.3
1,9-Ac_2AN	*EZsyn*	C_1	–844.78990701	93.33	96.19	25.88	–141.2	45.3	56.7	10.7	151.2	–6.5
							44.8	–128.4	48.1		151.1	6.8
1,10-Ac_2AN	*ZE*	C_1	–844.80536578	52.75	49.45	0.00	0.2	–180.0	1.0	1.8	150.1	0.2
							–108.0	73.0	75.3		151.6	–1.0
1,10-Ac_2AN	*ZZ*	C_1	–844.80575464	51.73	50.43	0.98	1.8	–178.2	2.7	2.4	150.1	0.0
							–65.9	115.1	68.5		151.4	1.0

1,10-Ac_2AN	*EZanti*	C_1	–844.80066416	65.09	63.37	13.91	148.6	–33.3	38.0	2.9	150.7	1.9
							–70.6	110.9	72.5		151.6	–1.5
1,10-Ac_2AN	*EEanti*	C_1	–844.80064430	65.14	63.38	13.92	148.5	–33.6	37.9	2.8	150.8	2.1
							–106.6	75.1	76.7		151.6	1.7
1,10-Ac_2AN	*EEsyn*	C_1	–844.80035871	65.89	63.70	14.25	149.9	–31.7	37.8	5.4	150.8	1.6
							111.3	–68.9	71.9		151.6	0.2
9,10-Ac_2AN	*E*	C_i	–844.79648217	76.07	71.57	0.00	–72.6	108.5	74.7	0.0	151.6	–1.1
9,10-Ac_2AN	[d] *E*	C_1	–	–	–	–	–85.0	94.0	86.7	1.6	151.3	–1.0
							87.0	–93.7	86.5		151.5	–0.6
9,10-Ac_2AN	*Z*	C_s	–844.79616186	76.91	71.63	0.06	71.8	–108.9	74.2	2.9	151.6	–0.7
9,10-Ac_2AN	*E*	C_2	–844.79637404	76.35	72.55	0.99	75.4	–105.7	76.9	0.1	151.6	–1.1
9,10-Ac_2AN	*Z*	C_2	–844.79619082	76.84	73.69	2.13	–71.9	108.8	73.9	3.1	151.6	–0.7
2,6-Ac_2AN	*EE*	C_{2h}	–844.82603788	–1.53	0.40	0.00	180.0	0.0	0.0	0.0	149.8	0.0
2,6-Ac_2AN	*ZE*	C_s	–844.82517129	0.75	0.79	0.40	0.0	180.0	0.0	0.0	150.1	0.0
							180.0	0.0			149.8	0.0
2,6-Ac_2AN	*ZZ*	C_{2h}	–844.82448815	2.54	4.19	3.79	0.0	–180.0	0.0	0.0	150.1	0.0
2,7-Ac_2AN	*EZ*	C_s	–844.82545585	0.00	0.00	0.00	180.0	0.0	0.0	0.0	149.7	0.0
							0.0	180.0			150.0	0.0
2,7-Ac_2AN	[d] *EZ*	C_1	–	–	–	–	171.9	–3.3	9.8	2.7	149.0	–4.8
							0.9	–178.8	1.6		148.9	0.3
2,7-Ac_2AN	*EE*	C_{2v}	–844.82612845	–1.77	0.20	0.20	180.0	0.0	0.0	0.0	149.8	0.0
2,7-Ac_2AN	*ZZ*	C_{2v}	–844.82444406	2.66	4.29	4.29	0.0	180.0	0.0	0.0	150.1	0.0
2,9-Ac_2AN	*EE*	C_1	–844.81120818	37.41	32.29	0.00	–178.9	1.4	2.1	1.6	149.8	–0.4
				1.50			–106.9	73.9	75.8		151.6	0.8
2,9-Ac_2AN	*EZ*	C_1	–844.81178130	35.90	35.90	3.61	–178.9	1.3	1.8	2.5	149.9	–0.2
				0.00			–63.0	118.1	66.2		151.3	1.1
2,9-Ac_2AN	*ZE*	C_1	–844.81042981	39.45	37.37	5.08	–1.8	178.5	2.6	1.8	150.1	–0.3
				3.55			–114.4	66.0	69.1		151.5	0.4
2,10-Ac_2AN	*EE*	C_1	–844.81146291	36.74	34.49	0.00	179.9	–0.7	0.7	1.8	149.7	0.5
							–113.9	66.7	70.5		151.5	–0.6
2,10-Ac_2AN	*EZ*	C_1	–844.81128488	37.21	34.81	0.32	179.6	–0.5	0.3	1.7	149.7	–0.1
					0.32		–68.8	112.0	71.4		151.5	0.9
2,10-Ac_2AN	*ZE*	C_1	–844.81074527	38.62	36.64	2.15	0.9	–179.8	1.9	2.0	150.0	0.7
					2.15		–114.3	66.4	69.3		151.4	–0.8
2,10-Ac_2AN	*ZZ*	C_1	–844.81084444	38.36	38.36	3.87	1.0	–179.2	1.7	2.1	150.0	–0.2
					3.87		–65.7	115.3	68.6		151.4	1.0

[a] $\tau_1(C^{9a}–C^1–C^{11}–O^{15})$ for 1-AcAN, 1,5-Ac_2AN, 1,6-Ac_2AN, 1,7-Ac_2AN and 1,8-Ac_2AN, $\tau_2(C^1–C^2–C^{11}–O^{15})$ for 2-AcAN and 2,7-Ac_2AN, $\tau_2(C^5–C^6–C^{13}–O^{16})$ for 1,6-Ac_2AN, $\tau_2(C^8–C^7–C^{13}–O^{16})$ for 1,7-Ac_2AN, $\tau_9(C^{9a}–C^9–C^{11}–O^{15})$ for 9-AcAN and 9,10-Ac_2AN.
[b] $\upsilon_1(C^2–C^1–C^{11}–O^{15})$ for 1-AcAN, 1,5-Ac_2AN, 1,6-Ac_2AN, 1,7-Ac_2AN and 1,8-Ac_2AN, $\upsilon_2(C^3–C^2–C^{11}–O^{15})$ for 2-AcAN and 2,7-Ac_2AN, $\upsilon_2(C^7–C^6–C^{13}–O^{16})$ for 1,6-Ac_2AN, $\upsilon_2(C^6–C^7–C^{13}–O^{16})$ for 1,7-Ac_2AN, $\upsilon_9(C^{8a}–C^9–C^{11}–O^{15})$ for 9-AcAN and 9,10-Ac_2AN.
[c] $C^1–C^{11}$ for 1-AcAN, 1,5-Ac_2AN, 1,6-Ac_2AN, 1,7-Ac_2AN and 1,8-Ac_2AN, $C^2–C^{11}$ for 2-AcAN and 2,7-Ac_2AN, $C^6–C^{13}$ for 1,6-Ac_2AN, $C^7–C^{13}$ for 1,7-Ac_2AN, $C^9–C^{11}$ for 9-AcAN and 9,10-Ac_2AN.
[d] the selected geometrical parameters derived from the corresponding X-ray structures.

Table 6. Total energies (E_{Tot}), relative energies (ΔE_{Tot}) and Gibbs free energies (ΔG_{298}) and selected geometric parameters of mono- and diacetylanthracenes.

Ketone 1-AcAN adopts a C_s-*Z* conformation as its global minimum. The planar (excluding the methyl hydrogens) C_s-1*Z*-AcAN is overcrowded due to the short $O^{13}\cdots H^9$ contact distance (the $O^{13}\cdots H^9$ distance is 215 pm, 14% penetration, based on the sum of the wan-der-Vaals

radii of oxygen and hydrogen, 244 pm [Zefirov, 1997]). The non-planar C_1-1*E*-AcAN conformation (the twist angle $\tau_1(C^{9a}–C^1–C^{11}–O^{13})$=150.8°) is higher in energy by 13.0 kJ/mol. The energy barrier for the *E*,*Z*-diastereomerization C_s-1*Z*-AcAN→C_1-1*E*-AcAN by the rotation of the acetyl group via a nearly orthogonal transition state is 19.5 kJ/mol. As mentioned above, 1-AcAN [Langer1993] crystallizes as the *Z*-diastereomer, which is correctly described by the calculated structure of C_s-1*Z*-AcAN. However, the carbonyl group in the crystal structure of 1-AcAN is considerably twisted out of the plane of the anthracene ring system, τ_1=27.1°. As a result, the calculated C_s-1*Z*-AcAN structure is more overcrowded than the X-ray structure (in the latter the $O^{13}\cdots H^9$ distance is 223 pm).

Ketone 2-AcAN adopts a C_s-*E* conformation as its global minimum. Its local minimum C_s-2*Z*-AcAN conformation is 2.2 kJ/mol higher in energy. Both conformations are not overcrowded, lacking any *peri*-interactions. The energy barrier for the *E*,*Z*-diastereomerization C_s-2*E*-AcAN→C_s-2*Z*-AcAN by the rotation of the acetyl group via a nearly orthogonal transition state is 31.5 kJ/mol. The calculated C_s-2*E*-AcAN conformation corresponds well to the *E*-conformation of the crystal structure. The latter, however, features a small twist angle of $\tau_2(C^1–C^2–C^{11}–O^{13})$=173.1°, in contrast to the planar (excluding the methyl hydrogens) calculated structure.

In the global minimum conformation of 9-AcAN the twist angle $\tau_9(C^{9a}–C^9–C^{11}–O^{13})$ is –67.0°. This conformations cannot be defined as either *E* or *Z*, and no other minimum conformation was located. Comparing the calculated structure of 9-AcAN with the crystal structure of 9-AcAN reported in the literature [Zouev2011], the carbonyl group in the latter is almost orthogonal to the plane of the anthracene ring system: the twist angle $\tau_9(C^{9a}–C^9–C^{11}–O^{13})$=87.9° is considerably larger than the twist angle predicted by the DFT calculations. The energy barrier for the enantiomerization of 9-AcAN via the orthogonal [C_s-9-AcAN] transition state is only 3.6 kJ/mol. The low enantiomerization barrier as compared to the diastereomerization barriers in 1-AcAN and 2-AcAN is due to an already high twist angle in 9-AcAN.

Ketone 1,5-Ac_2AN adopt a C_{2h}-1*Z*,5*Z* conformation as its global minimum. The geometry optimizations under C_2 or C_i symmetry constraints converged to the C_{2h} symmetry structure. C_{2h}-1*Z*,5*Z*-Ac_2AN is considerably overcrowded due to the short $O^{15}\cdots H^9/O^{16}\cdots H^{10}$ contact distances (14% penetration). The C_{2h}-1*Z*,5*Z*-Ac_2AN conformation corresponds to the *Z*,*Z* X-ray structure of 1,5-Ac_2AN. However, the calculated structure is planar (excluding the methyl hydrogens), while the X-ray structure has the twist angle $\tau_1(C^{9a}–C^1–C^{11}–O^{15})$=20.0° and the dihedral angle θ=22.7°, and, as a result, is less overcrowded. In addition to the global minimum, there are three local minima conformations of 1,5-Ac_2AN: C_1-1*Z*,5*E*-Ac_2AN, C_i-1*E*,5*E*-*anti*-Ac_2AN and C_2-1*E*,5*E*-*syn*-Ac_2AN. The four conformations of 1,5-Ac_2AN undergo diastereomerizations by the rotation of one of the acetyl groups via "nearly orthogonal" transition states, in which the rotating acetyl group has the twist angle of τ=85–97°, and the other acetyl group retains its *E*- or *Z*-conformation. The rotation of an acetyl group of C_{2h}-1*Z*,5*Z*-Ac_2AN via [C_1-1*Z*,90-Ac_2AN] leads to the C_1-1*Z*,5*E*-Ac_2AN conformation, which is 12.8 kJ/mol higher in energy than the global minimum. The *E*-orientation of the acetyl group at the 5-position and the *peri*-interactions of its methyl hydrogens with H^{10} force the acetyl group out of the aromatic plane, thus decreasing the conjugation. Due to the twist angle $\tau_1(C^{10a}–C^5–C^{13}–O^{16})$=152.4° which differs from either 0° or 180°, rotation of the 1*Z*-acetyl group of C_1-1*Z*,5*E*-Ac_2AN may be realized in either *anti*- (via [C_1-90,5*E*-*anti*-Ac_2AN]) or in *syn*-direction (via [C_1-90,5*E*-*syn*-Ac_2AN]) relative to the 5*E*-acetyl group. These processes lead to the different local minima C_i-1*E*,5*E*-*anti*-Ac_2AN and C_2-1*E*,5*E*-*syn*-Ac_2AN conformations, respectively, which are 27.4 and 28.0 kJ/mol higher in

energy than C_{2h}-1*Z*,5*Z*-Ac_2AN, due to both acetyl groups being forced out of the aromatic plane: $\tau_1(C^{9a}–C^1–C^{11}–O^{15})$=150.6° and 151.9°, respectively. In addition, the C_i-1*E*,5*E*-*anti*-Ac_2AN and C_2-1*E*,5*E*-*syn*-Ac_2AN conformations may undergo *syn*,*anti*-diastereomerization via the [C_1-1*E*,5E_{180}-Ac_2AN] transition state. It is a "nearly planar" transition state of a different type than the "nearly orthogonal" ones; the twist angle of the rotating acetyl group is close to zero, and the other acetyl group retains its *E*- or *Z*-conformation. The [C_1-1*E*,5E_{180}-Ac_2AN] transition state is considerably strained due to the short $O^{16}...H^{10}$ distance (205.3 pm) and the distorted sp^2 angles $C^{13}–C^5–C^{10a}$ (127.9°) and $C^{13}–C^5–C^6$ (113.4°). The diastereomerization processes in 1,5-Ac_2AN are shown in Fig. 19.

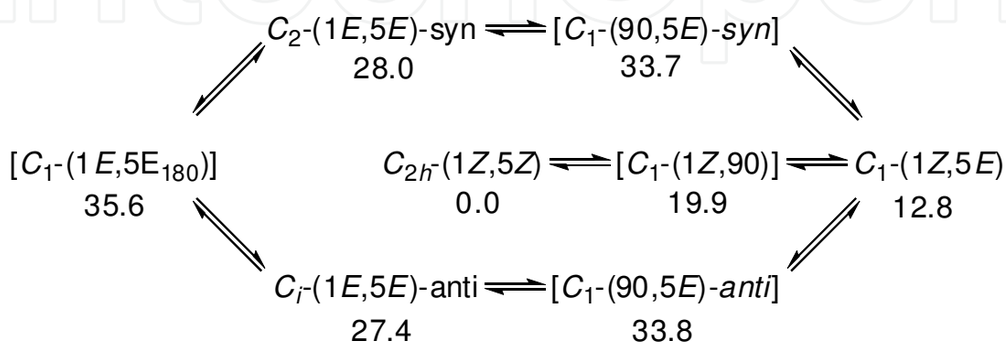

Fig. 19. The interconversion of conformations of 1,5-Ac_2AN and their relative Gibbs free energies (ΔG_{298}, kJ/mol)

Ketone 1,6-Ac_2AN adopts a C_s-1*Z*,6*E* conformation as its global minimum. Like C_{2h}-1*Z*,5*Z*-Ac_2AN, it is overcrowded due to the short $O^{15}...H^9$ contact distance (14% penetration). The C_s-1*Z*,6*E*-Ac_2AN conformation corresponds to the *Z*,*E* X-ray structure of 1,6-Ac_2AN. As in the case of 1,5-Ac_2AN, the DFT calculations predict a planar structure for 1,6-Ac_2AN, while the X-ray geometry features the twisted 1*Z*-acetyl group: the twist angle $\tau_1(C^{9a}–C^1–C^{11}–O^{15})$=30.0° and the dihedral angle θ=32.2°. The 6*E*-acetyl group remains in the aromatic plane in both calculated and the X-ray geometries. The rotation of the 1*Z*-acetyl group leads from C_s-1*Z*,6*E*-Ac_2AN via [C_1-90,6*E*-Ac_2AN] to the local minimum C_1-1*E*,6*E*-Ac_2AN, which is 13.6 kJ/mol higher in energy. The 6*E*-acetyl group, in contrast to the 1*E*-acetyl group, lies in the aromatic plane: $\tau_1(C^{9a}–C^1–C^{11}–O^{15})$=150.6° and $\tau_2(C^5–C^6–C^{13}–O^{16})$=179.9°. The rotation of the 6*E*-acetyl group of C_1-1*E*,6*E*-Ac_2AN may be realized either via [C_1-1*E*,90-*syn*-Ac_2AN] or via [C_1-1*E*,90-*anti*-Ac_2AN] transition states; both pathways lead to C_1-1*E*,6*Z*-*anti*-Ac_2AN, which is 15.4 kJ/mol higher in energy than the global minimum. The rotation of the 6*E*-acetyl group in C_s-1*Z*,6*E*-Ac_2AN via [C_1-1*Z*,90-Ac_2AN] leads to the local minimum C_s-1*Z*,6*Z*-Ac_2AN, which is only 1.7 kJ/mol higher in energy than the global minimum. The rotation of the 1*E*-acetyl group in C_1-1*E*,6*Z*-Ac_2AN via [C_1-90,6*Z*-Ac_2AN] also leads to C_s-1*Z*,6*Z*-Ac_2AN. The diastereomerization processes in 1,6-Ac_2AN are shown in Fig. 20.

Ketone 1,7-Ac_2AN, similarly to 1,6-Ac_2AN, adopts a C_s-1*Z*,7*E* conformation as its global minimum. It is overcrowded due to the short $O^{15}...H^9$ contact distance (15% penetration). The C_s-1*Z*,7*E*-Ac_2AN conformation corresponds to the *Z*,*E* X-ray structure of 1,7-Ac_2AN. The differences between the geometries of the planar DFT calculated structure of C_s-(1*Z*,7*E*)-Ac_2AN and the twisted X-ray structure of 1,7-Ac_2AN are smaller than in 1,5-Ac_2AN and 1,6-Ac_2AN. In the X-ray structure of 1,7-Ac_2AN the twist angles are $\tau_1(C^{9a}–C^1–C^{11}–O^{15})$=-15.2°

and $\tau_2(C^8–C^7–C^{13}–O^{16})$=-176.6. The relative stabilities of the conformations of 1,7-Ac_2AN and its conformational space are very similar to those of 1,6-Ac_2AN, both being α,β-diacetylanthracenes. The local minima conformations C_s-1*Z*,7*E*-Ac_2AN, C_1-1*E*,7*E*-Ac_2AN and C_1-1*E*,7*Z*-*anti*-Ac_2AN are higher in energy than the global minimum by 3.5, 14.5, and 16.6 kJ/mol, respectively. The diastereomerization processes in 1,7-Ac_2AN are shown in Fig. 21.

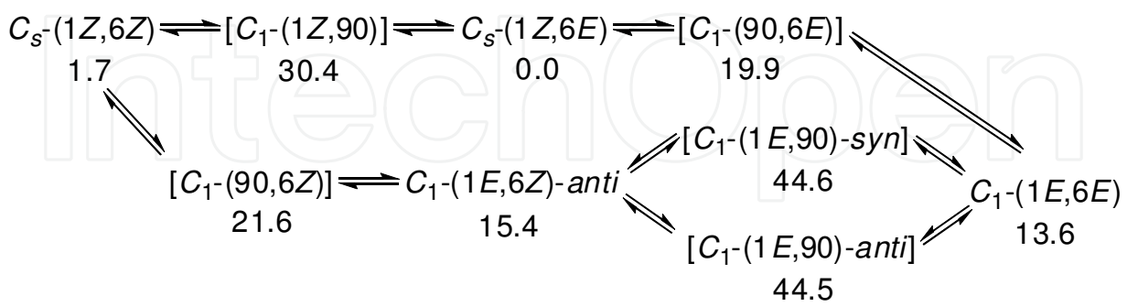

Fig. 20. The interconversion of conformations of 1,6-Ac_2AN and their relative Gibbs free energies (ΔG_{298}, kJ/mol)

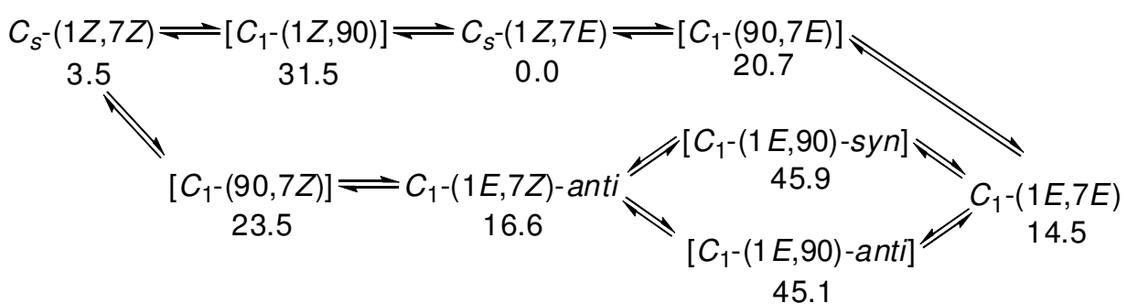

Fig. 21. The interconversion of conformations of 1,7-Ac_2AN and their relative Gibbs free energies (ΔG_{298}, kJ/mol)

The most interesting diacetylanthracene is 1,8-Ac_2AN. *Peri*-interactions $O^{15}\cdots H^9$ and $O^{16}\cdots H^9$ tilt both carbonyl groups out of the aromatic plane, rendering a planar conformation such as C_{2h}-1Z,5Z-Ac_2AN energetically highly unfavorable. Ketone 1,8-Ac_2AN adopts a C_2-1Z,8Z-*anti* conformation as its global minimum. It is overcrowded due to the short $O^{15}\cdots H^9$ contact distance (12% penetration). The C_2-1Z,8Z-*anti*-Ac_2AN conformation corresponds to the *Z,Z* X-ray structure of 1,8-Ac_2AN. Both structures feature twisted carbonyl groups; however, in the X-ray structure the twist angles are more pronounced ($\tau_1(C^{9a}–C^1–C^{11}–O^{15})$=-32.4° and -34.0°, θ=35.4° and 36.0°) than in the calculated structure ($\tau_1(C^{9a}–C^1–C^{11}–O^{15})$=-17.3°, θ=19.3°). Although the conformational space of 1,8-Ac_2AN resembles that of another α,α-diacetylanthracene, 1,5-Ac_2AN, it is more complicated. There are three local minima conformations of 1,8-Ac_2AN: C_1-1Z,8*E*-Ac_2AN, C_s-1*E*,8*E*-*syn*-Ac_2AN and C_2-1*E*,8*E*-*anti*-Ac_2AN. Rotation of an acetyl group of C_2-1Z,8Z-Ac_2AN via [C_1-1Z,90-Ac_2AN] leads to the C_1-1Z,8*E*-Ac_2AN conformation, which is only 0.4 kJ/mol higher in energy. The tilting of the 8*E*-acetyl group ($\tau_2(C^{8a}–C^8–C^{13}–O^{16})$=150.4°) allows the 1*Z*-acetyl group to align itself with the aromatic plane ($\tau_1(C^{9a}–C^1–C^{11}–O^{15})$=1.5°), restoring the conjugation and thus stabilizing this conformation. The rotation of the 1*Z*-acetyl group of C_1-1Z,8*E*-Ac_2AN may be realized

in either *syn*- (via [C_1-90,8*E*-*syn*-Ac_2AN]) or in *anti*-direction (via [C_1-90,8*E*-*anti*-Ac_2AN]) relative to the 8*E*-acetyl group. These pathways lead to the local minima C_s-1*E*,8*E*-*syn*-Ac_2AN and C_2-1*E*,8*E*-*anti*-Ac_2AN conformations, respectively, which are 17.6 and 17.7 kJ/mol higher in energy than the global minimum. These two conformations undergo interconversion via the [C_1-1*E*,8E_{180}-Ac_2AN] transition state. The diastereomerization processes in 1,8-Ac_2AN are shown in Fig. 22.

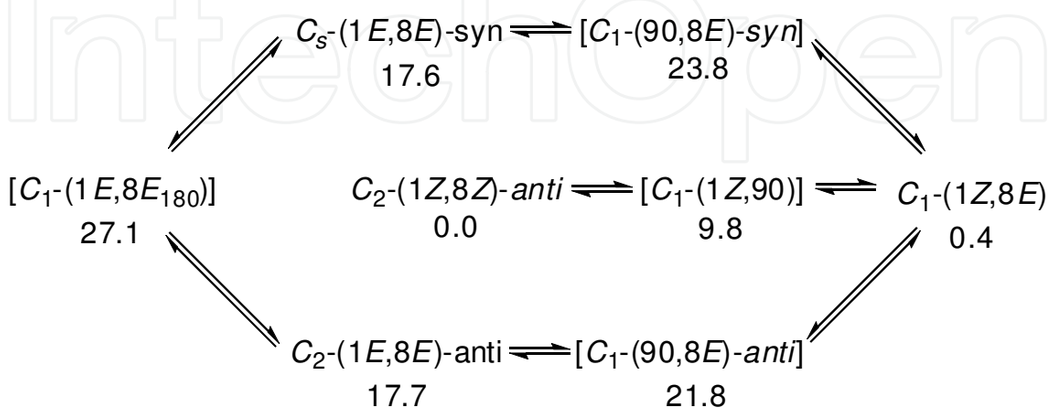

Fig. 22. The interconversion of conformations of 1,8-Ac_2AN and their relative Gibbs free energies (ΔG_{298}, kJ/mol)

Ketone 2,7-Ac_2AN adopts a C_s-2*E*,7*Z* conformation as its global minimum. It is not overcrowded, lacking *peri*-interactions. The C_s-(2*E*,7*Z*)-Ac_2AN conformation corresponds well to the *E,Z* X-ray structure of 2,7-Ac_2AN. The differences between the geometries of the planar DFT calculated structure of C_s-2*E*,7*Z*-Ac_2AN and the twisted X-ray structure of 2,7-Ac_2AN are not large: in the latter structure the twist angles are $\tau_2(C^1–C^2–C^{11}–O^{15})$=171.9° and $\tau_2(C^8–C^7–C^{13}–O^{16})$=0.9° (θ=9.8° and 1.6°, respectively). There are only two local minima conformations of 2,7-Ac_2AN, both are planar like the global minimum. Due to the twist angles τ_2 being either 0° or 180°, no *anti*-, *syn*-conformations are possible. The rotation of the 7*Z*-acetyl group in C_s-2*E*,7*Z*-Ac_2AN via [C_1-2*E*,90-Ac_2AN] leads to C_{2v}-2*E*,7*E*-Ac_2AN conformation, which is only 0.2 kJ/mol higher in energy. The rotation of the 2*E*-acetyl group of C_s-2*E*,7*Z*-Ac_2AN via [C_1-90,7*Z*-Ac_2AN] leads to the C_{2v}-2*Z*,7*Z*-Ac_2AN conformation, which is 4.3 kJ/mol higher in energy than the global minimum. The diastereomerization processes in 2,7-Ac_2AN are shown in Fig. 23.

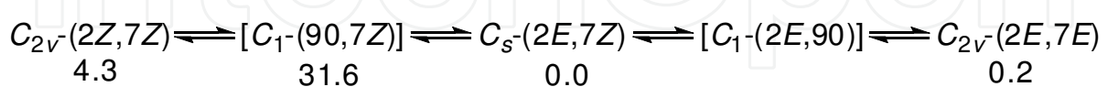

Fig. 23. The interconversion of conformations of 2,7-Ac_2AN and their relative Gibbs free energies (ΔG_{298}, kJ/mol)

The conformational space of 2,6-Ac_2AN is similar to that of 2,7-Ac_2AN. The global minimum is the C_{2h}-2*E*,6*E*-Ac_2AN conformation. Rotation of the 6*E*-acetyl group leads to C_s-2*E*,6*Z*-Ac_2AN conformation, which is only 0.4 kJ/mol higher in energy than the global minimum. The rotation of the 2*E*-acetyl group in C_s-2*E*,6*Z*-Ac_2AN leads to C_{2h}-2*Z*,6*Z*-Ac_2AN conformation, which is 3.8 kJ/mol higher in energy than the global minimum. The diastereomerization processes in 2,6-Ac_2AN are shown in Fig. 24.

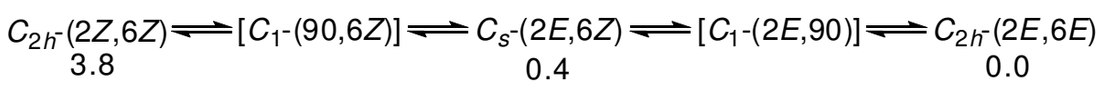

Fig. 24. The interconversion of conformations of 2,6-Ac_2AN and their relative Gibbs free energies (ΔG_{298}, kJ/mol)

Ketone 9,10-Ac_2AN stands out of the other diacetylanthracenes by virtue of its acetyl groups being each flanked by two *peri*-hydrogens. In order to avoid short non-contact distances to $H^1/H^4/H^5/H^8$, the acetyl groups in all the conformations of 9,10-Ac_2AN are considerably twisted. Another mode for the relief of the steric strain in 9,10-Ac_2AN is elongation of the C^{11}–C^9 and C^{12}–C^{10} carbonyl bonds, 151.6 pm, as compared to 149.7 pm in planar C_s-(2E,7Z)-Ac_2AN and 149.8 pm in C_s-(2E,6E)-Ac_2AN. The global minimum of 9,10-Ac_2AN is a C_i-E conformation, with the twist angles $\tau_9(C^{9a}–C^9–C^{11}–O^{15})=–72.6°$, $\tau_9(C^{10a}–C^{10}–C^{13}–O^{16})=72.6°$ and the dihedral angle $\theta=74.7°$. It corresponds well to the X-ray structure, which features even higher twist angles $\tau_9=–85.0°$, 87.0° and the dihedral angles $\theta=86.7°$, 86.5°. The local minima conformations of 9,10-Ac_2AN are C_s-Z (0.1 kJ/mol), C_2-E (1.0 kJ/mol) and C_2-Z (2.1 kJ/mol). They all have high twist angles, ±71.8°, 75.4° and –71.9°, respectively. The similarity of the energies and the geometries of the four conformations of 9,10-Ac_2AN stems from the fact that in 9,10-Ac_2AN, each of the Z and E conformations is defined relative to the other acetyl group, and not by the twist angles of the carbonyl groups relative to the anthracene system, which are very similar for all four conformations of 9,10-Ac_2AN. The C_i-E global minimum undergoes diastereomerization to the C_2-E conformation via [C_1-(9E,10E_{180})] transition state, in which one of the carbonyl groups lies in the aromatic plane. The C_s-Z and C_2-Z conformations interconvert via the analogous [C_1-(9Z,10Z_0)] transition state. The C_i-E conformation diastereomerizes to the C_2-Z conformation and the C_2-E conformation diastereomerizes to the C_s-Z conformation via the pair of transition states [C_1-90-*syn*] and [C_1-90-*anti*], in which one of the carbonyl groups is orthogonal to the aromatic plane. The diastereomerization processes in 9,10-Ac_2AN are shown in Fig. 25.

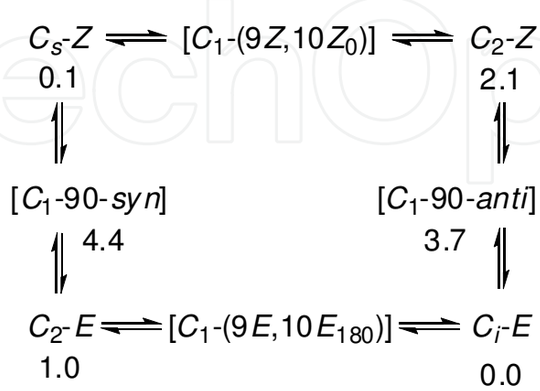

Fig. 25. The interconversion of conformations of 9,10-Ac_2AN and their relative Gibbs free energies (ΔG_{298}, kJ/mol)

Ketone 1,9-Ac_2AN has never been isolated. Recently 1,9-Ac_2AN has been claimed to be a putative intermediate in the Friedel–Crafts acyl rearrangements of 1,5-Ac_2AN, 1,8-Ac_2AN and 9,10-Ac_2AN in PPA to give 3-methylbenz[de]anthracen-1-one [Mala'bi et al., 2011]. Ketone 1,9-Ac_2AN adopts a C_1-1*Z*,9*Z*-*anti* conformation as its global minimum. Both acetyl groups are considerably twisted because of their mutual *peri*-positions: $\tau_1(C^{9a}–C^1–C^{11}–O^{15})$=–50.9°, $\tau_9(C^{9a}–C^9–C^{13}–O^{16})$=–59.6°. The local minimum conformation C_1-1*E*,9*Z*-*syn*-Ac_2AN is considerably higher in energy than the global minimum, 25.9 kJ/mol. Potentially, two more conformations may exist due to the twist angles τ_1 and τ_9 being different from 0° or 180°, i.e. C_1-1*Z*,9*Z*-*syn*-Ac_2AN and C_1-1*E*,9*Z*-*anti*-Ac_2AN. However, the search after these conformations has not resulted in any additional stationary points. The C_1-1*Z*,9*E*-Ac_2AN and C_1-1*E*,9*E*-Ac_2AN conformations have also not been found in the conformational space of 1,9-Ac_2AN, probably due to the considerable steric strain caused by the *peri*-interactions between the methyl of the 9*E*-acetyl group and the 1-acetyl group.

Ketone 1,10-Ac_2AN (which has never been synthesized [Mala'bi et al., 2011]) adopts a C_1-1*Z*,10*E* conformation as its global minimum. Contrary to 1,9-Ac_2AN, its acetyl groups do not affect directly each other. Hence, their twist angles, $\tau_1(C^{9a}–C^1–C^{11}–O^{15})$=0.2°, $\tau_9(C^{4a}–C^{10}–C^{13}–O^{16})$=–108.0°, are very close to the twist angles of the lone acetyl groups in C_s-1*Z*-AcAN (0.0°) and C_1-9-AcAN (–67.0°), respectively. Another consequence of the non-interacting acetyl groups in 1,10-Ac_2AN is the abundance of conformations – six minima conformations have been identified. The local minimum C_1-1*Z*,10*Z*-Ac_2AN conformation is only 1.0 kJ/mol less stable than the global minimum, and differs from it in the twist angle $\tau_9(C^{4a}–C^{10}–C^{13}–O^{16})$=–65.9°. There are four 1*E* conformations of 1,10-Ac_2AN, which have the twist angles $\tau_1(C^{9a}–C^1–C^{11}–O^{15})$ of 148–150° and the relative energy of 13.9–15.3 kJ/mol. The conformational behavior of 1,10-Ac_2AN is complicated. Depending on the rotational direction of the

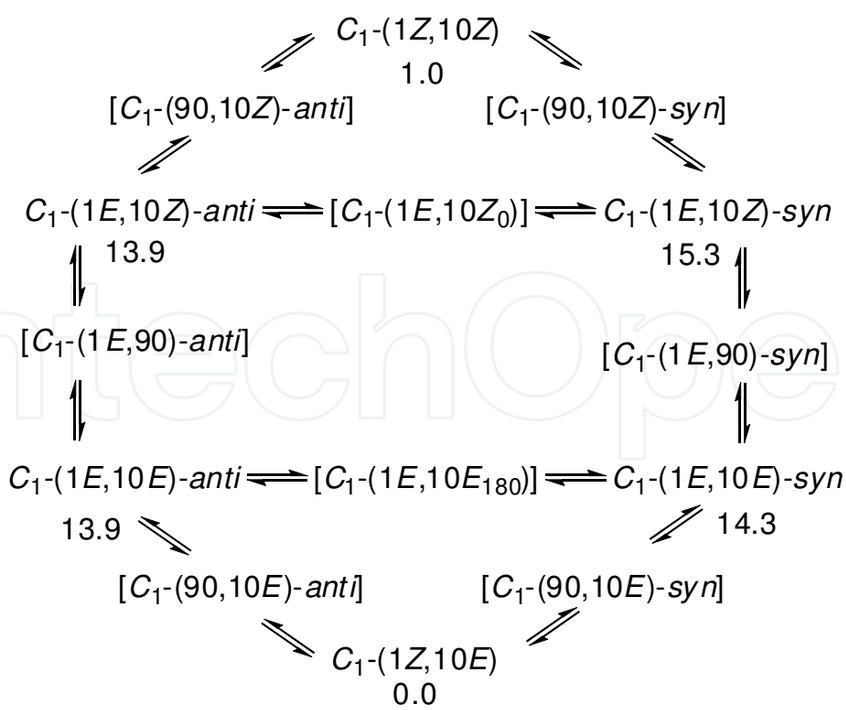

Fig. 26. The interconversion of conformations of 1,10-Ac_2AN and their relative Gibbs free energies (ΔG_{298}, kJ/mol)

1*Z*-acetyl group, the C_1-1*Z*,10*E*-Ac_2AN conformation may undergo diastereomerization to either C_1-1*E*,10*E*-*anti*-Ac_2AN or C_1-1*E*,10*E*-*syn*-Ac_2AN via the respective "nearly orthogonal" transition states. Analogously, C_1-1*Z*,10*Z*-Ac_2AN may undergo diastereomerization to either C_1-1*E*,10*Z*-*anti*-Ac_2AN or C_1-1*E*,10*Z*-*syn*-Ac_2AN. The C_1-1*E*,10*E*-*anti*-Ac_2AN and C_1-1*E*,10*Z*-*anti*-Ac_2AN conformations are interconnected via the [C_1-1*E*,90-*anti*-Ac_2AN] transition state, while C_1-1*E*,10*E*-*syn*-Ac_2AN and C_1-1*E*,10*Z*-*syn*-Ac_2AN are interconnected via the [C_1-1*E*,90-*syn*-Ac_2AN] transition state. Finally, C_1-1*E*,10*E*-*anti*-Ac_2AN is interconnected with C_1-1*E*,10*E*-*syn*-Ac_2AN and C_1-1*E*,10*Z*-*anti*-Ac_2AN is interconnected with C_1-1*E*,10*Z*-*syn*- Ac_2AN, via the "nearly planar" transition states [C_1-1*E*,10E_{180}-Ac_2AN] and [C_1-1*E*,10Z_0-Ac_2AN], respectively. The diastereomerization processes in 1,10-Ac_2AN are shown in Fig. 26.

Ketone 2,9-Ac_2AN (which has never been synthesized) adopts a C_1-2*E*,9*E* conformation as its global minimum. The acetyl groups in 2,9-Ac_2AN do not affect directly one another, and twist angles are similar to the respective twist angles in 2-AcAN and 9-AcAN: $\tau_2(C^1–C^2–C^{11}–O^{15})$=–178.9° and $\tau_9(C^{4a}–C^{10}–C^{13}–O^{16})$=–106.9°. There are two local minima conformations of 2,9-Ac_2AN, C_1-2*E*,9*Z*-Ac_2AN (3.6 kJ/mol above the global minimum) and C_1-2*Z*,9*E*-Ac_2AN (5.1 kJ/mol). Surprisingly, the search after the C_1-2*Z*,9*Z*-Ac_2AN conformation was not successful. The acetyl groups in the putative C_1-2*Z*,9*Z*-Ac_2AN conformation are not expected to cause a steric hindrance more severe than in the C_1-1*Z*,9*Z*-*anti*-Ac_2AN conformation. Nevertheless, the latter conformation exists and even was found to be a global minimum, while the former does not seem to exist. The global minimum C_1-2*E*,9*E*-Ac_2AN conformation may diastereomerize either to the C_1-2*E*,9*Z*-Ac_2AN conformation via the [C_1-2*E*,90-Ac_2AN] transition state, or to the C_1-2*Z*,9*E*-Ac_2AN conformation via the [C_1-90,9*E*-Ac_2AN] transition state. The diastereomerization processes in 2,9-Ac_2AN are shown in Fig. 27.

$$\underset{3.6}{C_1\text{-}(2E,9Z)} \rightleftharpoons [C_1\text{-}(2E,90)] \rightleftharpoons \underset{0.0}{C_1\text{-}(2E,9E)} \rightleftharpoons [C_1\text{-}(90,9E)] \rightleftharpoons \underset{5.1}{C_1\text{-}(2Z,9E)}$$

Fig. 27. The interconversion of conformations of 2,9-Ac_2AN and their relative Gibbs free energies (ΔG_{298}, kJ/mol)

Ketone 2,10-Ac_2AN (which has never been synthesized) adopts a C_1-2*E*,10*E* conformation as its global minimum. The twist angles are $\tau_2(C^1–C^2–C^{11}–O^{15})$=179.9° and $\tau_9(C^{4a}–C^{10}–C^{13}–O^{16})$=–113.9°. The global minimum C_1-2*E*,10*E*-Ac_2AN conformation may diastereomerize either to the C_1-2*Z*,10*E*-Ac_2AN conformation (the relative energy of 2.1 kJ/mol) via the [C_1-90,10*E*-Ac_2AN] transition state, or to the C_1-2*E*,10*Z*-Ac_2AN conformation (0.3 kJ/mol) via the [C_1-2*E*,90-Ac_2AN] transition state. Both these local minima configurations undergo diastereomerization to the C_1-2*Z*,10*Z*-Ac_2AN conformation (3.9 kJ/mol) via the [C_1-2*Z*,90-Ac_2AN] and [C_1-90,10*Z*-Ac_2AN] transition states, respectively. The diastereomerization processes in 2,10-Ac_2AN are shown in Fig. 28.

The comparison between the X-ray structures of mono- and diacetylanthracenes and their respective calculated geometries deserves a brief discussion. The absolute values of the twist angles of the B3LYP/6-31G(d) calculated conformations (including the local minima conformations) of mono- and diacetylanthracenes may be summarized as follows: $|\tau_1|$=0–17.3°[2] for the 1*Z*-acetyl groups, $|\tau_1|$=141.2–152.4° for the 1*E*-acetyl groups, $|\tau_2|$=0.0–1.8° for

[2] The 1,9-Ac_2AN is an outlier, having unusually high twist angle of the 1*Z*-acetyl group, $|\tau_1|$=51.9°, due to the steric strain caused by its interaction with the *peri* 9*Z*-acetyl group. The mutual *peri*-positions of the acetyl groups lead to an enhanced degree of overcrowding.

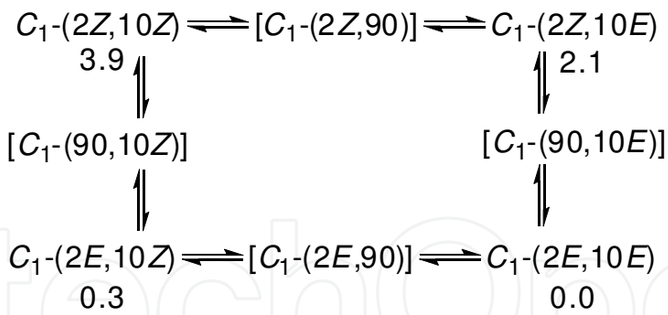

Fig. 28. The interconversion of conformations of 2,10-Ac_2AN and their relative Gibbs free energies (ΔG_{298}, kJ/mol)

the 2*Z*-acetyl groups, $|\tau_2|$=178.9–180.0° for the 2*E*-acetyl groups, and $|\tau_9|$=44.8–75.4° (180–$|\tau_9|$ values were taken for $|\tau_9|$>90°). The respective twist angles derived from the X-ray structures are $|\tau_1|$=15.2–34.0° for the 1*Z*-acetyl groups, $|\tau_2|$=0.9° for the 2*Z*-acetyl group, $|\tau_2|$=177.9–178.6° for the 2*E*-acetyl groups, and $|\tau_9|$=85.0–87.9°. There is no X-ray structure of acetylanthracenes featuring a 1*E*-acetyl group, and such conformations are always found to be local minima by the DFT calculations. The B3LYP/6-31G(d) calculations seem to underestimate the twist angles of the 1*Z*- and 9-acetyl groups in mono- and diacetylanthracenes. In a number of cases it leads to predicting planar and more overcrowded conformations than the respective twisted X-ray geometries. There is a limited number of reports in the literature that DFT methods, including B3LYP, could overstabilize planar conformations of biphenyl and related heteroaromatic compounds [Viruela et al., 1997; Karpfen et al., 1997]. As in the X-ray structures, the acetyl groups and the anthracene systems in the mono- and diacetylanthracenes under study are essentially planar. Thus, B3LYP/6-31G(d) satisfactorily predicts the overall conformations of mono- and diacetylanthracenes under study, i.e. the *Z*-conformation of 1-AcAN, the *E*-conformation of 2-AcAN, the twisted conformation of 9-AcAN, the *Z*,*Z* conformations of 1,5-Ac_2AN and 1,8-Ac_2AN, the *Z*,*E* conformations of 1,6-Ac_2AN, 1,7-Ac_2AN and 2,7-Ac_2AN, and the *E*,*E* conformation of 9,10-Ac_2AN. It has not escaped our mind, however, that the packing interactions in crystals can readily dominate and suppress any preference for one conformation or another, especially in the cases of low diastereomerization barriers and low energy differences. We also note the limitations of the DFT calculations in the gas phase and in the comparison of the computational results with the crystal structures.

The relative free Gibbs energies of the diacetylanthracenes under study are given in Table 6. It should be noted that 1,5-Ac_2AN is 11.2 kJ/mol more stable than its constitutional isomer 1,8-Ac_2AN. The acetyl groups of 1,5-Ac_2AN are attached to a starred and an unstarred aromatic carbons of alternant anthracene, while the acetyl groups of 1,8-Ac_2AN are both attached to starred aromatic carbons. Simple resonance considerations would favor the stabilization of 1,8-Ac_2AN over 1,5-Ac_2AN, due to the better delocalization of the partial positive charge in the dipolar Kekulé structures. However, the twist angle of the acetyl groups in 1,8-Ac_2AN are notably larger than that in 1,5-Ac_2AN, in both the crystal structures (32.4°/34° vs. 20.0°) and the DFT calculated geometries (17.3° vs. 0.0°). This increased twist angle decreases the conjugation between the acetyl group and the aromatic system, thus destabilizing 1,8-Ac_2AN relative to 1,5-Ac_2AN.

The order of stabilities of the global minima of the diacetylanthracenes is 2,7-Ac_2AN≈2,6-Ac_2AN>1,7-Ac_2AN≈1,6-Ac_2AN>1,5-Ac_2AN>2,9-Ac_2AN>2,10-Ac_2AN>1,8-Ac_2AN>1,10-Ac_2AN>>1,9-Ac_2AN>9,10-Ac_2AN. The acetyl groups at positions 1, 5 and 8 destabilize the diacetylanthracenes, while acetyl groups at positions 9 and 10 cause even greater destabilization. The destabilization of the 1, 5, 8, 9 and 10-substituted diacetylanthracenes relative to their 2, 6 and 7-substituted constitutional isomers stems from the overcrowding due to repulsive non-bonding interactions between the carbonyl oxygen/methyl group and the aromatic hydrogens in *peri*-positions, and from the decreased resonance stabilization between the carbonyl and the aromatic system. Thus, the acetyl groups in 9,10-Ac_2AN, 1,9-Ac_2AN, 1,10-Ac_2AN and 1,8-Ac_2AN, being considerably tilted out of the aromatic plane, reduce the relative stabilities of these diacetylanthracenes, potentially allowing deacylation, transacylation and acyl rearrangements. By contrast, 2,7-Ac_2AN and 2,6-Ac_2AN are not expected to undergo the Friedel–Crafts acyl rearrangements.

2.3.2 Activation barriers

As noted above, monoacetylanthracenes and diacetylanthracenes may undergo *E*,*Z*-diastereomerizations and *syn*,*anti*-diastereomerizations by rotation of their acetyl groups. The diastereomerization of the first type connects an *E*-diastereomer with a *Z*-diastereomer and proceeds via a "nearly orthogonal" transition state, in which the acetyl group, rotating around the C_{arom}–C_{carb} bond, has the twist angle of τ=85–97° (the other acetyl group in diacetylanthracenes retains its *E*- or *Z*-orientation). The diastereomerization of the second type occurs only in diacetylanthracenes and connects either an *E*-*syn*-diastereomer with an *E*-*anti*-diastereomer, or a *Z*-*syn*-diastereomer with a *Z*-*anti*-diastereomer. It proceeds via a "nearly planar" transition states, in which the twist angle of the rotating acetyl group is close to either 180° (*E*-diastereomer) or zero (*Z*-diastereomer), and the other acetyl group retains its *E*- or *Z*-orientation. Fig. 29 and Fig. 30 show the *E*,*Z*-diastereomerization and *syn*,*anti*-diastereomerization on the example of 1,8-Ac_2AN.

Table 7 gives the energy barriers for the *E*,*Z*-diastereomerization and *syn*,*anti*-diastereomerization in the monoacetylanthracenes and diacetylanthracenes under study by rotation of the acetyl groups via the respective nearly orthogonal or nearly planar transition states. The E,Z-diastereomerization energy barriers may be divided into three groups, depending on the position of the acetyl group that undergoes rotation and on its conformation. *E*-Acetyl groups at positions 1, 5 and 8 and acetyl groups at positions 9 and 10 have the lowest energy barriers, 3.6–9.5 kJ/mol, due to their already significant twist angles (τ=141–152° for *E*-acetyl groups at positions 1, 5 and 8 and τ=67–73° for acetyl groups at positions 9 and 10). *Z*-Acetyl groups at the same positions 1, 5 and 8 have medium energy barriers, 19.5–23.5 kJ/mol. The twist angles of these acetyl groups are smaller (τ=0–17°), but the *E*,*Z*-diastereomerization in this case is facilitated by the steric strain due to repulsive *peri*-interactions between the carbonyl oxygen and aromatic H^9/H^{10} hydrogens. Finally, both *E*- and *Z*-acetyl groups at positions 2, 6 and 7 have the highest energy barriers for diastereomerization, 27.3–31.6 kJ/mol, due to the lack of steric strain and negligible twist angles (less than 1°). For comparison, the experimental rotational energy barrier for methyl 1-(2-methylnaphthyl) ketone is 33.9 kJ/mol (–110 °C, [Wolf, 2008]). Table 8 gives the relative Gibbs free energies of the global minima and the most stable local minima of the acetylanthracenes whose crystal structures have been determined in this study or reported in the literature, i.e. 1-AcAN, 2-AcAN, 9-AcAN, 1,5-Ac_2AN, 1,6-Ac_2AN, 1,7-Ac_2AN, 1,8-Ac_2AN, 2,7-Ac_2AN and 9,10-Ac_2AN, as well the energy barriers for their *E*,*Z*-

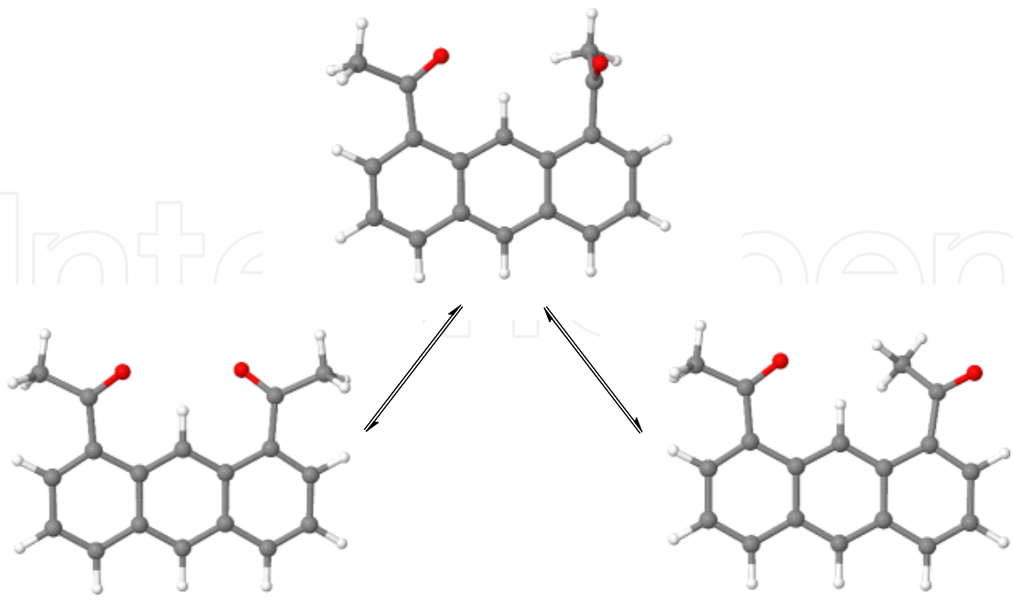

Fig. 29. *E*,*Z*-Diastereomerization of C_2-1*Z*,8*Z*-Ac_2AN to C_2-1*Z*,8*E*-Ac_2AN via [1*Z*,90-Ac_2AN] transition state

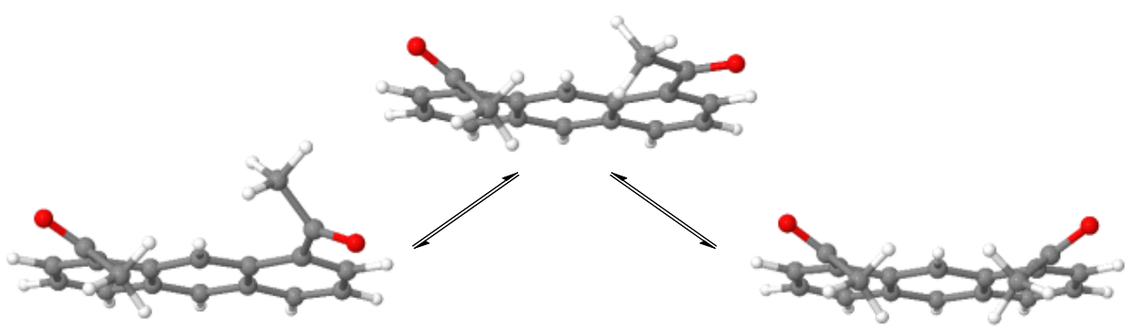

Fig. 30. *syn*,*anti*-Diastereomerization of C_2-1*E*,8*E*-*anti*-Ac_2AN to C_s-1*E*,8*E*-*syn*-Ac_2AN via [1*E*,8E_{180}-Ac_2AN] transition state

diastereomerizations. The energy barriers are in the range of 20–32 kJ/mol (relative to the respective global minima) for the rotation of the acetyl groups at 1, 2, 5, 6 and 7 positions. The lower energy barrier in 1,8-Ac_2AN (9.8) may be rationalized by destabilization of the global minimum due to the larger twist of the acetyl groups. This effect is even more pronounced in the case of 9-AcAN and 9,10-Ac_2AN, which have large twist values (67° and 73°, respectively) and remarkably low *E*,*Z*-diastereomerization barriers (less than 4 kJ/mol). All these barriers are sufficiently low to allow a swift *E*,*Z*-diastereomerizations on the NMR time scale (at room temperature), in accordance with the results of the NMR experiments (*vide supra*). The differences in the relative energies of the global minimum and the most stable local minimum of these acetylanthracenes are relatively small, 0.06-3.5 kJ/mol (with the exception of 1-AcAN and 1,5-Ac_2AN), which suggests the presence of both *E*- and *Z*-diastereomers in equilibrium mixture at ambient temperature.

E,*Z* diastereomerization or *syn*,*anti*-diastereomerization	ΔG‡ kJ/mol	Transition state	E_{Tot} Hartree
1*Z*-AcAN→1*E*-AcAN	19.52	[1-AcAN]	–692.16527547
1*E*-AcAN→1*Z*-AcAN	6.51		
2*Z*-AcAN→2*E*-AcAN	29.28	[2-AcAN]	–692.16644237
2*E*-AcAN→2*Z*-AcAN	31.52		
9-AcAN→9-AcAN*	3.64[a]	[9-AcAN]	–692.16355087
1*Z*,5*Z*-Ac_2AN→1*Z*,5*E*-Ac_2AN	19.93	[1*Z*,90-Ac_2AN]	–844.80776475
1*Z*,5*E*-Ac_2AN→1*Z*,5*Z*-Ac_2AN	7.14		
1*E*,5*E*-*syn*-Ac_2AN→1*E*,5*E*-*anti*-Ac_2AN	7.54	[1*E*,5E_{180}-Ac_2AN]	–844.80415197
1*E*,5*E*-*anti*-Ac_2AN→1*E*,5*E*-*syn*-Ac_2AN	8.22		
1*Z*,5*E*-Ac_2AN→1*E*,5*E*-*syn*-Ac_2AN	20.93	[90,5*E*-*syn*-Ac_2AN]	–844.80261144
1*E*,5*E*-syn-Ac_2AN→1*Z*,5*E*-Ac_2AN	5.67		
1*Z*,5*E*-Ac_2AN→1*E*,5*E*-*anti*-Ac_2AN	21.01	[90,5*E*-*anti*-Ac_2AN]	–844.80259178
1*E*,5*E*-*anti*-Ac_2AN→1*Z*,5*E*-Ac_2AN	6.44		
1*Z*,6*Z*-Ac_2AN→1*Z*,6*E*-Ac_2AN	28.66	[1*Z*,90-Ac_2AN]	–844.80884650
1*Z*,6*E*-Ac_2AN→1*Z*,6*Z*-Ac_2AN	30.35		
1*Z*,6*Z*-Ac_2AN→1*E*,6*Z*-Ac_2AN	19.86	[90,6*Z*-Ac_2AN]	–844.81218832
1*E*,6*Z*-Ac_2AN→1*Z*,6*Z*-Ac_2AN	6.13		
1*Z*,6*E*-Ac_2AN→1*E*,6*E*-Ac_2AN	19.86	[90,6*E*-Ac_2AN]	–844.81289093
1*E*,6*E*-Ac_2AN→1*Z*,6*E*-Ac_2AN	6.29		
1*E*,6*Z*-Ac_2AN→1*E*,6*E*-Ac_2AN	29.02	[1*E*,90-*anti*-Ac_2AN]	–844.80381925
1*E*,6*E*-Ac_2AN→1*E*,6*Z*-Ac_2AN	30.88		
1*E*,6*Z*-Ac_2AN→1*E*,6*E*-Ac_2AN	29.16	[1*E*,90-*syn*-Ac_2AN]	–844.80371345
1*E*,6*E*-Ac_2AN→1*E*,6*Z*-Ac_2AN	31.01		
1*Z*,7*Z*-Ac_2AN→1*Z*,7*E*-Ac_2AN	28.05	[1*Z*,90-Ac_2AN]	–844.80879074
1*Z*,7*E*-Ac_2AN→1*Z*,7*Z*-Ac_2AN	31.54		
1*Z*,7*Z*-Ac_2AN→1*E*,7*Z*-Ac_2AN	19.95	[90,7*Z*-Ac_2AN]	–844.81202172
1*E*,7*Z*-Ac_2AN→1*Z*,7*Z*-Ac_2AN	6.83		
1*Z*,7*E*-Ac_2AN→1*E*,7*E*-Ac_2AN	20.72	[90,7*E*-Ac_2AN]	–844.81303091
1*E*,7*E*-Ac_2AN→1*Z*,7*E*-Ac_2AN	6.26		
1*E*,7*Z*-Ac_2AN→1*E*,7*E*-Ac_2AN	28.53	[1*E*,90-*anti*-Ac_2AN]	–844.80384032
1*E*,7*E*-Ac_2AN→1*E*,7*Z*-Ac_2AN	30.69		
1*E*,7*Z*-Ac_2AN→1*E*,7*E*-Ac_2AN	29.29	[1*E*,90-*syn*-Ac_2AN]	–844.80370612
1*E*,7*E*-Ac_2AN→1*E*,7*Z*-Ac_2AN	31.45		
1*Z*,8*Z*-*anti*-Ac_2AN→1*Z*,8*E*-Ac_2AN	9.81	[1*Z*,90-Ac_2AN]	–844.80732674
1*Z*,8*E*-Ac_2AN→1*Z*,8*Z*-*anti*-Ac_2AN	9.46		

1*E*,8*E*-*anti*-Ac_2AN→1*Z*,8*E*-Ac_2AN	4.15	[90,8*E*-*anti*-Ac_2AN]	–844.80278079
1*Z*,8*E*-Ac_2AN→1*E*,8*E*-*anti*-Ac_2AN	21.46		
1*E*,8*E*-*syn*-Ac_2AN→1*Z*,8*E*-Ac_2AN	6.22	[90,8*E*-*syn*-Ac_2AN]	–844.80231227
1*Z*,8*E*-Ac_2AN→1*E*,8*E*-*syn*-Ac_2AN	23.46		
1*E*,8*E*-*syn*-Ac_2AN→1*E*,8*E*-*anti*-Ac_2AN	9.49	[1*E*,8E_{180}-Ac_2AN]	–844.80296243
1*E*,8*E*-*anti*-Ac_2AN→1*E*,8*E*-*syn*-Ac_2AN	9.42		
C_i-*E*-9,10-Ac_2AN→C_2-*Z*-9,10-Ac_2AN	3.73	[C_1-90-*anti*-9,10-Ac_2AN]	–844.79633239
C_2-*Z*-9,10-Ac_2AN→C_i-*E*-9,10-Ac_2AN	3.67		
C_2-*E*-9,10-Ac_2AN→C_s-*Z*-9,10-Ac_2AN	3.44	[C_1-90-*syn*-9,10-Ac_2AN]	–844.79605863
C_s-*Z*-9,10-Ac_2AN→C_2-*E*-9,10-Ac_2AN	4.36		
C_s-2*E*,7*Z*-Ac_2AN→C_s-2*Z*,7*Z*-Ac_2AN	31.63	[C_1-90,7Z-Ac_2AN]	–844.81338779
C_s-2*Z*,7*Z*-Ac_2AN→C_s-2*E*,7*Z*-Ac_2AN	27.34		

[a] enantiomerization barrier

Table 7. Energy barriers ($\Delta G^{\ddagger}$, kJ/mol) for diastereomerizations of monoacetylanthracenes and diacetylanthracenes

			ΔG_{298}	$\Delta\Delta G_{298}$	$\Delta G^{\ddagger}$
1-AcAN	*Z*	C_s	15.79	0.00	19.52
1-AcAN	*E*	C_1	28.80	13.01	6.51
2-AcAN	*E*	C_s	0.00	0.00	31.52
2-AcAN	*Z*	C_s	2.24	2.24	29.28
9-AcAN	–	C_1	36.94	0.00	3.64
1,5-Ac_2AN	*ZZ*	C_{2h}	27.69	0.00	19.93
1,5-Ac_2AN	*ZE*	C_1	40.48	12.79	7.14
1,6-Ac_2AN	*ZE*	C_s	13.45	0.00	30.35
1,6-Ac_2AN	*ZZ*	C_s	15.14	1.69	28.66
1,7-Ac_2AN	*ZE*	C_s	12.34	0.00	31.54
1,7-Ac_2AN	*ZZ*	C_s	15.83	3.50	28.05
1,8-Ac_2AN	*ZZ*	C_2	38.89	0.00	9.81
1,8-Ac_2AN	*EZ*	C_1	39.25	0.35	9.46
9,10-Ac_2AN	*E*	C_i	71.57	0.00	3.73
9,10-Ac_2AN	*Z*	C_s	71.63	0.06	3.67
2,7-Ac_2AN	*EZ*	C_s	0.00	0.00	31.63

Table 8. Relative energies (ΔG_{298} and $\Delta\Delta G_{298}$, kJ/mol) of selected monoacetylanthracenes and diacetylanthracenes and respective energy barriers for *E*,*Z*-diastereomerizations ($\Delta G^{\ddagger}$, kJ/mol)

3. Conclusions

The monoacetylanthracenes and diacetylanthracenes under study adopt non-planar conformations in their crystal structures. The twist angles are maximal for the 9-acetyl groups ($|\tau_9|$=85.0–87.9°) and significant for the 1Z-acetyl groups ($|\tau_1|$=15.2–34.0°), but very small for 2-acetyl groups. The conformations in solution are in agreement with the X-ray crystal structure conformations, according to the NMR data. The crystal structures are stabilized by intermolecular interactions: aromatic–aromatic π–π interactions (1,6-Ac_2AN and 1,7-Ac_2AN), C···H-π interactions (2-AcAN, 1,5-Ac_2AN, 2,7-Ac_2AN and 9,10-Ac_2AN), or π–π interactions between the anthracene unit and the carbonyl bond (1,8-Ac_2AN). The B3LYP/6-31G(d) calculated conformations of the monoacetylanthracenes and diacetylanthracenes are in good agreement with the X-ray crystal structures. The acetyl groups in the crystal structures and the B3LYP/6-31G(d) calculated global minima of the monoacetylanthracenes and diacetylanthracenes preferentially adopts 1*Z* and 2*E* conformations. The order of stabilities of the diacetylanthracenes under study is 2,7-Ac_2AN>1,7-Ac_2AN≈1,6-Ac_2AN>1,5-Ac_2AN>1,8-Ac_2AN>9,10-Ac_2AN. The acetyl groups at positions 1, 5 and 8 destabilize the diacetylanthracenes because of the repulsive interactions between the carbonyl oxygen/methyl group and the aromatic *peri*-hydrogens, and because of the decreased resonance stabilization. This effect is even more pronounced for the acetyl groups at positions 9 and 10. The B3LYP/6-31G(d) calculated energy barriers for the E,Z-diastereomerizations show that the *E*,*Z*-diastereomerizations is swift on the NMR time scale (at room temperature), in accordance with the results of the NMR experiments. The present results of the crystallographic and theoretical study of monoacetylanthracenes and diacetylanthracenes contribute to our understanding of the motifs of reversibility and thermodynamic control in the Friedel–Crafts acyl rearrangements of these representative PAKs.

4. Experimental section

Table 9 summarizes the applied methods of preparation of the monoacetylanthracenes and diacetylanthracenes. Melting points are uncorrected. All NMR spectra were recorded with Bruker DRX 500 MHz spectrometer. ^{1}H-NMR spectra were recorded at 500.13 MHz using $CDCl_3$ as solvent and as internal standard, $\delta(CDCl_3)$=7.263 ppm. ^{13}C-NMR spectra were recorded at 125.75 MHz using $CDCl_3$ as a solvent with internal standard, $\delta(CDCl_3)$=77.008 ppm. Complete assignments were made through 2-dimensional correlation spectroscopy (COSY, HSQC, HBMC and NOESY). Anthracene and nitrobenzene were obtained from Sigma-Aldrich; acetyl chloride and aluminum chloride were obtained from Acros. All the solvents were AR grade. Chloroform and dichloromethane were distilled before use. Single crystal X-ray diffraction was carried out on a Bruker SMART APEX CCD X-ray diffractometer, equipped with graphite monochromator and using MoKα radiation (λ=0.71073 Å). Low temperature was maintained with a Bruker KRYOFLEX nitrogen cryostat. The diffractometer was controlled by a Pentium-based PC running the SMART software package [Bruker AXS GmbH, 2002a]. Immediately after collection, the raw data frames were transferred to a second PC computer for integration and reduction by the SAINT program package [Bruker AXS GmbH, 2002b]. The structures were solved and refined by the SHELXTL software package [Bruker AXS GmbH, 2002c].

Compound	Method of preparation	Solvent	Melting point °C	Lit. melting point, °C	Solvent of recryst.	Reference
1-AcAN	Anthracene $AlCl_3$, Acetyl chloride	CH_2Cl_2	110	109	EtOH	Bassilios, 1962 Mala'bi et al.,2009
2-AcAN	Anthracene $AlCl_3$, Acetyl chloride	$C_6H_5NO_2$	177	174–178	$MeCO_2Et$	Mala'bi et al.,2009 Bassilios, 1966
9-AcAN	Anthracene $AlCl_3$, Acetyl chloride	CH_2Cl_2	78	75–76	$MeCO_2Et$	Bassilios, 1962 Bassilios, 1962
1,5-Ac_2AN	Anthracene $AlCl_3$, Acetyl chloride	CH_2Cl_2	215	213	$CHCl_3$	Bassilios, 1963
1,6-Ac_2AN	2-AcAN $AlCl_3$, Acetyl chloride	ClC_2H_4Cl	170–172	171–172	$MeCO_2Et$	Gore, 1966
1,7-Ac_2AN	2-AcAN $AlCl_3$, Acetyl chloride	ClC_2H_4Cl	102–103	–	EtOH	–
1,8-Ac_2AN	Anthracene $AlCl_3$, Acetyl chloride	CH_2Cl_2	179	174–176	$CHCl_3$	Sarobe & Jenneskens, 1997
2,7-Ac_2AN	2-AcAN $AlCl_3$, Acetyl chloride	$C_6H_5NO_2$	156–157		*i*PrOH	
9,10-Ac_2AN	9,10-dicarbomethoxy-anthracene, MeLi	Et_2O	247	249–250	CH_2Cl_2	Duerr, 1988

Table 9. Summary of methods of preparation of monoacetylanthracenes and diacetylanthracenes.

The quantum mechanical calculations were performed using the Gaussian03 [Frisch et al., 2004] package. Becke's three parameter hybrid density functional B3LYP [Becke, 1993], with the non-local correlation functional of Lee, Yang, and Parr [Lee et al., 1988] was used. The split valence 6-31G(d) basis set [Hariharan & Pople, 1973] was employed. All structures were fully optimized using symmetry constrains as indicated. Vibrational frequencies were computed at the same level of theory to verify the nature of the stationary points. For calculating the thermal corrections to Gibbs' free energy, the zero point energies were scaled by 0.9804 [Bauschlicher & Partridge, 1995].

5. References

Adams, C. J., Earle, M. J., Roberts, G. & Seddon, K. R. (1998) Friedel–Crafts Reactions in Room Temperature Ionic Liquids. *Chemical Communications*, No. 19, pp. 2097–2098, ISSN: 1364-548X

Agranat, I. & Shih, Y.-S. (1974) Haworth Synthesis as a Route to the Anthracene Ring System. *Synthesis*, No. 12, pp. 865–867, ISSN: 0039-7881

Agranat, I. & Shih, Y.-S. (1974) The Synthesis of Linearly Annelated Polycyclic Ketones by Friedel-Crafts Rearrangements of Their Angular Isomers. *Synthetic Communications*, Vol. 4, No. 2, pp. 119–126, ISSN: 0039-7911

Agranat, I., Shih, Y.-S. & Bentor, Y. (1974) Incursion of reversibility in Friedel-Crafts acylations. *Journal of American Chemical Society*, Vol. 96, No. 4, pp. 1259–1260, ISSN: 0002-7863

Agranat, I., Bentor, Y. & Shih, Y.-S. (1977) Remarkable Reversibility in Aromatic Friedel-Crafts Acylations. *Para↔Ortho* Acyl Rearrangements of Fluorofluorenones in Polyphosphoric Acid. *Journal of the American Chemical Society*, Vol. 99, No. 21, pp. 7068–7070, ISSN: 0002-7863

Anderson, K., Becker, H., Engelhardt, L. M., Hansen, L. & White, A. H. (1984) Molecular geometry and crystal structure of 9-acetylanthracene. *Australian Journal of Chemistry*, Vol. 37, No. 6, pp. 1337–1340, ISSN: 0004-9425

Andreou, A. D., Gore, P. H. & Morris, D. F. C. (1978) Acetyl exchange between acetylmesitylene and acetyl chloride under Friedel–Crafts conditions. *Journal of Chemical Society*, *Chemical Communications*, No. 6, pp. 271–272, ISSN: 0022-4936

Assadi, N., Pogodin, S., Cohen, S., Levy, A. & Agranat, I. (2009) Overcrowded naphthologs of mono-bridged tetraarylethylenes: analogs of bistricyclic aromatic enes. *Structural Chemistry*, Vol. 20, pp.541–556, ISSN: 1040-0400

Balaban, A. T. (1966) Deacylation of Non-conjugated Ketones and the Reversibility of C-acylations, In: *Omagiu Acad. Prof. Raluca Ripan*, Dragulesea, C., pp 103–109, Editura Academiei Republicii Socialiste Romania, Bucharest

Bassilios, H.F., Shawky, M. & Salem A.Y. (1963) Acetylation of anthracene by the Friedel-Crafts reaction, using ethylene chloride as the solvent. *Recueil des Travaux Chimiques des Pays-Bas*, Vol. 82, No. 3, pp. 298–301, ISSN: 0165-0513

Bassilios, H.F., Salem, A.Y. & Anous, M.T. (1966) Acetylation of anthracene by the Friedel-Crafts reaction using nitrobenzene as the solvent. *Bulletin des Societes Chimiques Belges*, Vol. 75, No. 9-10, pp. 582–588, ISSN: 0037-9646

Bauschlicher Jr., C. W. & Partridge, H. (1995) A modification of the Gaussian-2 approach using density functional theory. *Journal of Chemical Physics*, Vol. 103., No. 5, pp. 1788–1791, ISSN: 0021-9606

Becke, A. D. (1993) Density-functional thermochemistry. III. The role of exact exchange. *Journal of Chemical Physics*, Vol. 98, No. 7, pp. 5648–5652, ISSN: 0021-9606

Biedermann, P. U., Stezowski, J. J. & Agranat, I. (2001) Thermochromism of overcrowded bistricyclic aromatic enes (BAEs). A theoretical study. *Chemical Communications*, No. 11, pp. 954–955, ISSN: 1364-548X

Brock, C. P. & Dunitz, J. D. (1990) Temperature Dependence of Thermal Motion in Crystalline Anthracene. *Acta Crystallographica Section B*, Vol. 46, No. 6, pp. 795–806, ISSN: 0108-7681

Bruker AXS GmbH (2002) SAINT-NT V5.0, D-76181 Karlsruhe, Germany

Bruker AXS GmbH (2002) SHELXTL-NT V6.1, D-76181 Karlsruhe, Germany

Bruker AXS GmbH (2002) SMART-NT V5.6, D-76181 Karlsruhe, Germany

Buehler, C. A. & Pearson, D. E. (1970). *Survey of Organic Synthesis*, p. 652, Wiley-Interscience, ISBN: 978-0894644085, New York

Dahl, T. (1994) The Nature of Stacking Interactions between Organic Molecules Elucidated by Analysis of Crystal Structures. *Acta Chemica Scandinavica*, Vol. 48, pp. 95–106, ISSN:0904-213X

de Proft, F. & Geerlings, P. (2001) Conceptual and Computational DFT in the Study of Aromaticity. *Chemical Reviews*, Vol. 101, No. 5, pp. 1451–1464, ISSN: 0009-2665

Desiraju, G. R. & Gavezzotti, A. (1989) Crystal Structures of Polynuclear Aromatic Hydrocarbons. Classification, Rationalization and Prediction from Molecular Structure. *Acta Crystallographica Section B: Structural Science,* Vol. 45, No. 5, pp. 473–482, ISSN: 0108-7681

Dowdy, D., Gore, P. H. & Waters, D. N. (1991) The Friedel–Crafts acetylation of naphthalene in 1,2-dichloroethane solution. Kinetics and mechanism. *Journal of Chemical Society, Perkin Transactions 2*, No. 8, pp. 1149–1159, ISSN: 1472-779X

Duerr, B.F., Chung Y.-S. & Czarnik, A.W. (1988) Syntheses of 9,10-Disubstituted Anthracenes Derived from 9,10-Dilithioanthracene. *Journal of Organic Chemistry*, Vol. 53, No. 9, pp. 2120-2122, ISSN: 0022-3263

Effenberger, F., Klenk, H. & Reiter, P. L. (1973) New Aspects of the Fries Rearrangement. *Angewandte Chemie International Edition*, Vol. 12, No. 9, pp. 775–776, ISSN: 1433-7851

Eliel, E. L. & Wilen, S. H. (1994) *Stereochemistry of Organic Compounds,* pp. 24–31, Wiley, ISBN: 978-0471016700, New York

Frangopol, M., Genunche, A., Frangopol, P. T. & Balaban, A. T. (1964) Pyrylium salts formed by diacylation of olefins XV: ^{14}C-tracer study of the acetylation of 4-chloro-3,4-dimethyl-2-pentanone. *Tetrahedron*, Vol. 20, No. 8, pp. 1881–1888, ISSN: 0040-4020

Frisch, M. J., Trucks, G. W., Schlegel, H. B., Scuseria, G. E., Robb, M. A., Cheeseman, J. R., Montgomery Jr., J. A., Vreven, T., Kudin, K. N., Burant, J. C., Millam, J. M., Iyengar, S. S., Tomasi, J., Barone, V., Mennucci, B., Cossi, M., Scalmani, G., Rega, N., Petersson, G. A., Nakatsuji, H., Hada, M., Ehara, M., Toyota, K., Fukuda, R., Hasegawa, J., Ishida, M., Nakajima, T., Honda, Y., Kitao, O., Nakai, H., Klene, M., Li, X., Knox, J. E., Hratchian, H. P., Cross, J. B., Adamo, C., Jaramillo, J., Gomperts, R., Stratmann, R. E., Yazyev, O., Austin, A. J., Cammi, R., Pomelli, C., Ochterski, J. W. , Ayala, P. Y., Morokuma, K., Voth, G. A., Salvador, P., Dannenberg, J. J., Zakrzewski, V. G., Dapprich, S., Daniels, A. D., Strain, M. C., Farkas, O., Malick, D. K., Rabuck, A. D., Raghavachari, K., Foresman, J. B., Ortiz, J. V., Cui, Q., Baboul, A. G., Clifford, S., Cioslowski, J., Stefanov, B. B., Liu, G., Liashenko, A., Piskorz, P., Komaromi, I., Martin, R. L., Fox, D. J., Keith, T., Al-Laham, M. A., Peng, C. Y., Nanayakkara, A., Challacombe, M. Gill, P. M. W., Johnson, B., Chen, W., Wong, M. W., Gonzalez, C. & Pople, J. A. (2004) *Gaussian 03, Revision C.02*, Gaussian, Inc., Wallingford CT.

Gore, P. H. (1955) The Friedel-Crafts Acylation Reaction and its Application to Polycyclic Aromatic Hydrocarbons. *Chemical Review*, Vol. 55, No. 2, pp. 229–281, ISSN: 0009-2665

Gore, P. H. (1964) In: *Friedel–Crafts and Related Reactions*, Olah, G. A., Vol. 3 (Part 1), pp. 1–381, Wiley-Interscience, ISBN: 978-0470653241, New York

Gore, P. H. (1974). Friedel-Crafts acylations: some unusual aspects of selectivity. *Chemistry & Industry*, Vol. 18, pp. 727–731, ISSN: 0009-3068

Gore, P.H. & Thadani, C.K. (1966) The Formation of Mono- and Di-ketones in the Friedel-Crafts Acetylation of Anthracene. *Journal of the Chemical Society (C)*. No. pp. 1729–1733, ISSN: 0022-4952

Hariharan, P. C. & Pople, J. A. (1973) The Influence of Polarization Functions on Molecular Orbital Hydrogenation Energies. *Theoretica Chimica Acta*, Vol. 28, pp. 213–222, ISSN: 0040-5744

Heaney, H. (1991) The Intramolecular Aromatic Friedel–Crafts Reaction In: *Comprehensive Organic Synthesis*, Trost, B. M., Fleming, I., Heathcock, C. H., Vol. 2, pp. 753–768, Pergamon Press, ISBN: 978-0-08-052349-1, Oxford.

Hunter, C. A., Singh, J. & Thornton, J. M. (1991) π–π Interactions: the Geometry and Energetics of Phenylalanine-Phenylalanine Interactions in Proteins. *Journal of Molecular Biology*, Vol. 218, No. 4, pp. 837–846, ISSN: 00222836

Janiak, C. (2000) A critical account on π–π stacking in metal complexes with aromatic nitrogen-containing ligands. *Journal of the Chemical Society, Dalton Transactions*, No. 21, pp. 3885–3896, ISSN: 1477-9226

Karpfen, A., Choi, C. H. & Kertesz, M. (1997) Single-Bond Torsional Potentials in Conjugated Systems: A Comparison of ab Initio and Density Functional Results. *Journal of Physical Chemistry A*, Vol. 101, No. 40, pp. 7426–7433, ISSN: 1089-5639

Koch, W. & Holthausen, M.C. (2001) *A Chemist Guide to Density Functional Theory* (2nd Ed), Wiley-VCH, ISBN: 3-527-30372-3, Weinheim.

Langer, V. & Becker, H.-D. (1993) Crystal structure of 1-acetylanthracene, $C_{16}H_{12}O$. *Zeitschrift für Kristallographie*, Vol. 206, No. 1, pp. 155–157, ISSN: 0044-2968

Lee, C., Yang, W. & Parr, R. G. (1988) Development of the Colle-Salvetti correlation-energy formula into a functional of the electron density. *Physical Review B*, Vol. 37, No. 2, pp. 785–789, ISSN: 1098-0121

Levy, L., Pogodin, S., Cohen, S. & Agranat, I. (2007) Reversible Friedel–Crafts Acylations of Phenanthrene: Rearrangements of Acetylphenanthrenes. *Letters in Organic Chemistry*, Vol. 4, No. 5, pp. 314–318, ISSN: 1570-1786

Li, M.-Q. & Jing, L.-H. (2006) 1,5-Diacetylanthracene. *Acta Crystallographica Section E*, Vol. 62, No. 9, pp. o3852–o3853, ISSN: 1600-5368

Mala'bi, T., Pogodin, S. & Agranat, I. (2009) Reversible Friedel-Crafts Acylations of Anthracene: Rearrangements of Acetylanthracenes. *Letters in Organic Chemistry*, Vol. 6, No. 3, pp. 237–241, ISSN: 1570-1786

Mala'bi, T., Pogodin, S. & Agranat, I. (2011) Kinetic control wins out over thermodynamic control in Friedel–Crafts acyl rearrangements. *Tetrahedron Letters*, Vol. 52, No. 16, pp. 1854–1857, ISSN: 0040-4039

Martin, N. H., Allen III, N. W., Brown, J. D., Kmiec, D. M. Jr. & Vo, L. (2003) An NMR shielding model for protons above the plane of a carbonyl group. *Journal of Molecular Graphics and Modelling*, Vol. 22, No. 1, pp. 127–131, ISSN: 1093-3263

McConnell, H. M. (1957) Theory of Nuclear Magnetic Shielding in Molecules. I. Long-Range Dipolar Shielding of Protons. *Journal of Chemical Physics*, Vol. 27, No. 1, pp. 226-229, ISSN: 0021-9606

Moss, G. P. (1996) Basic Terminology of Stereochemistry (IUPAC recommendations 1996). *Pure & Applied Chemistry*, Vol. 68, No. 12, pp. 2193–2222, ISSN: 0033-4545; http://www.chem.qmul.ac.uk/iupac/stereo.

Muller, P. (1994) Glossary of Terms Used in Physical Organic Chemistry (IUPAC Recommendations 1994). *Pure & Applied Chemistry*, Vol. 66, No. 5, pp. 1077–1184, ISSN: 0033-4545

Murugan, N. A. & Jha, P. C. (2009) Pressure dependence of crystal structure and molecular packing in anthracene. *Molecular Physics*, Vol. 107, No. 16, 1689–1695, ISSN: 0026-8976

Nenitzescu, C. D. & Balaban, A. T. (1964) In: *Friedel–Crafts and Related Reactions*; Olah, G. A., Vol. 3 (part 2), pp. 1033–1152, Wiley-Interscience, ISBN: 978-0470653265, New York.

Norman, R. O. C. & Taylor, R. (1965). *Electrophilic Substitution in Benzenoid Compounds*, p. 174–182, Elsevier, ISBN: 978-0444404275, London

Okamoto, A. & Yonezawa, N. (2009) Reversible ArS_E Aroylation of Naphthalene Derivatives. *Chemistry Letters*, Vol. 38, No. 9, pp. 914–915, ISSN: 0366-7022

Olah, G. A. (1973). *Friedel–Crafts Chemistry*, p. 102, Wiley-Interscience, ISBN: 0471653152, New York

Pearson, D. E. & Buehler, C. A. (1971). Unusual Electrophilic Aromatic Substitution in Synthesis. *Synthesis*, No. 9, pp. 455–477, ISSN: 0039-7881

Pogodin, S., Rae, I. D. & Agranat, I. (2006) The Effects of Fluorine and Chlorine Substituents across the Fjords of Bifluorenylidenes: Overcrowding and Stereochemistry. *European Journal of Organic Chemistry*, No. 22, pp. 5059–5068, ISSN: 1434-193X

Sarobe, M. & Jenneskens, L.W. (1997) High-Temperature Behavior of 1,8-Diethynylanthracene. Benz[*mno*]aceanthrylene, a Transient Intermediate for Cyclopenta[*cd*]pyrene. *Journal of Organic Chemistry*, Vol. 62, pp. 8247–8250, ISSN: 0022-3263

Sinclair, V. C., Robertson, J. M. & Mathieson, A. McL. (1950) The Crystal and Molecular Structure of Anthracene. II. Structure Investigation by the Triple Fourier Series Method. *Acta Crystallographica*, Vol. 3, No. 4, pp. 251–256, ISSN: 0365-110X

Sinnokrot, M. O. & Sherrill, C. D. (2006) High-Accuracy Quantum Mechanical Studies of π–π Interactions in Benzene Dimers. *Journal of Physical Chemistry A*, Vol. 110, No. 37, pp. 10656–10668, ISSN: 1089-5639

Titinchi, S. J. J., Kamounah, F. S., Abbo, H. S. & Hammerich, O. (2008) The synthesis of mono- and diacetyl-9*H*-fluorenes. Reactivity and selectivity in the Lewis acid catalyzed Friedel-Crafts acetylation of 9*H*-fluorene. *ARKIVOC*, No. xiii, pp. 91–105, ISSN: 1551-7004

Viruela, P. M., Viruela, R., Ortí, E. & Brédas, J.-L. (1997) Geometric Structure and Torsional Potential of Biisothianaphthene. A Comparative DFT and ab Initio Study. *Journal of the American Chemical Society*, Vol. 119, No. 6, pp. 1360–1369, ISSN: 0002-7863

Wang, Z. (2009). Friedel-Crafts Acylation, In: *Comprehensive Organic Name Reactions and Reagents*, Vol. 1, Chapt. 248, pp. 1126–1130, Wiley, ISBN: 978-0471704508, New York

Wolf, C. (2008) *Dynamic Stereochemistry of Chiral Compounds. Principles and Applications*, pp. 95-96, RSC Publishing, ISBN: 978-0-85404-246-3, Washington.

Zefirov, Y. V. (1997) Comparative Analysis of Systems of van der Waals Radii. *Crystallography Reports (Kristallografiya)*, Vol. 42, No. 1, pp. 111–116, ISSN: 1063-7745

Zouev, I., Cao, D.-K., Sreevidya, T. V., Telzhensky, M., Botoshansky, M. & Kaftory, M. (2011) Photodimerization of anthracene derivatives in their neat solid state and in solid molecular compounds. *CrystEngComm*, Vol. 13, No. 13, pp. 4376–4381, ISSN: 1466-8033

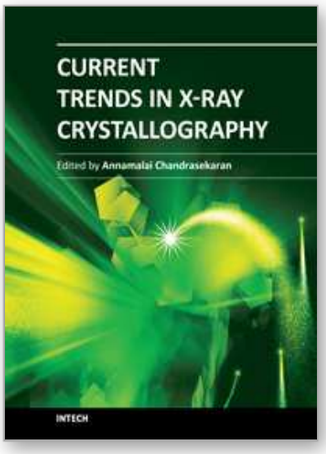

Current Trends in X-Ray Crystallography

Edited by Dr. Annamalai Chandrasekaran

ISBN 978-953-307-754-3

Hard cover, 436 pages

Publisher InTech

Published online 16, December, 2011

Published in print edition December, 2011

This book on X-ray Crystallography is a compilation of current trends in the use of X-ray crystallography and related structural determination methods in various fields. The methods covered here include single crystal small-molecule X-ray crystallography, macromolecular (protein) single crystal X-ray crystallography, and scattering and spectroscopic complimentary methods. The fields range from simple organic compounds, metal complexes to proteins, and also cover the meta-analyses of the database for weak interactions.

How to reference

In order to correctly reference this scholarly work, feel free to copy and paste the following:

Sergey Pogodin, Shmuel Cohen, Tahani Mala'bi and Israel Agranat (2011). Polycyclic Aromatic Ketones – A Crystallographic and Theoretical Study of Acetyl Anthracenes, Current Trends in X-Ray Crystallography, Dr. Annamalai Chandrasekaran (Ed.), ISBN: 978-953-307-754-3, InTech, Available from: http://www.intechopen.com/books/current-trends-in-x-ray-crystallography/polycyclic-aromatic-ketones-a-crystallographic-and-theoretical-study-of-acetyl-anthracenes

INTECH
open science | open minds

InTech Europe
University Campus STeP Ri
Slavka Krautzeka 83/A
51000 Rijeka, Croatia
Phone: +385 (51) 770 447
Fax: +385 (51) 686 166
www.intechopen.com

InTech China
Unit 405, Office Block, Hotel Equatorial Shanghai
No.65, Yan An Road (West), Shanghai, 200040, China
中国上海市延安西路65号上海国际贵都大饭店办公楼405单元
Phone: +86-21-62489820
Fax: +86-21-62489821